FLINOVIA IV

FLOW-**I**NDUCED-**N**OISE AND **V**IBRATION **I**SSUES AND **A**SPECTS

UNSW Sydney 22-24 May 2023

Hosted by the Flow Noise Group
School of Mechanical and Manufacturing Engineering

https://conference.unsw.edu.au/en/Flinovia

Proudly supported by

Australian Government
Defence

Welcome and Orientation

Welcome to Sydney, UNSW and Flinovia IV! We are looking forward to your participation.

Venue

Flinovia IV will be held in the design suite in the Ainsworth Building (Building J17) on the Kensington Campus. Please see the campus map for details (also in this booklet).

Take the lift or stairs to Level 5 in Building J17 (Ainsworth), where we will greet you.

Getting to UNSW

UNSW Sydney is located in Kensington. If you are coming from Central station or the CBD, you can catch the Light Rail to campus. There are two Light Rail stops to UNSW. You can catch the L2 Randwick Light Rail service to the UNSW High St stop, which is opposite our Gate 9 entrance or you can catch the L3 Kingsford Light Rail service to the UNSW Anzac Parade stop, located at the lower campus entrance to UNSW on Anzac Parade.

There are also a number of bus services you can catch to the UNSW campus from Central station and the CBD.

More Getting to UNSW Information

Public Transport Information

Sydney Public Transport runs using the OPAL card or your own Debit/Credit Card. Just tap your credit card before and after your ride.

More information on public transport is here.

Information on contactless payments using your credit or debit card

Speaker's Dinner Information

Café Sydney
5th Floor, Customs House
31 Alfred Street, Circular Quay, NSW, 2000

Make own way to Venue by Public Transport or Taxi

Website: https://cafesydney.com/

Kensington Campus Map

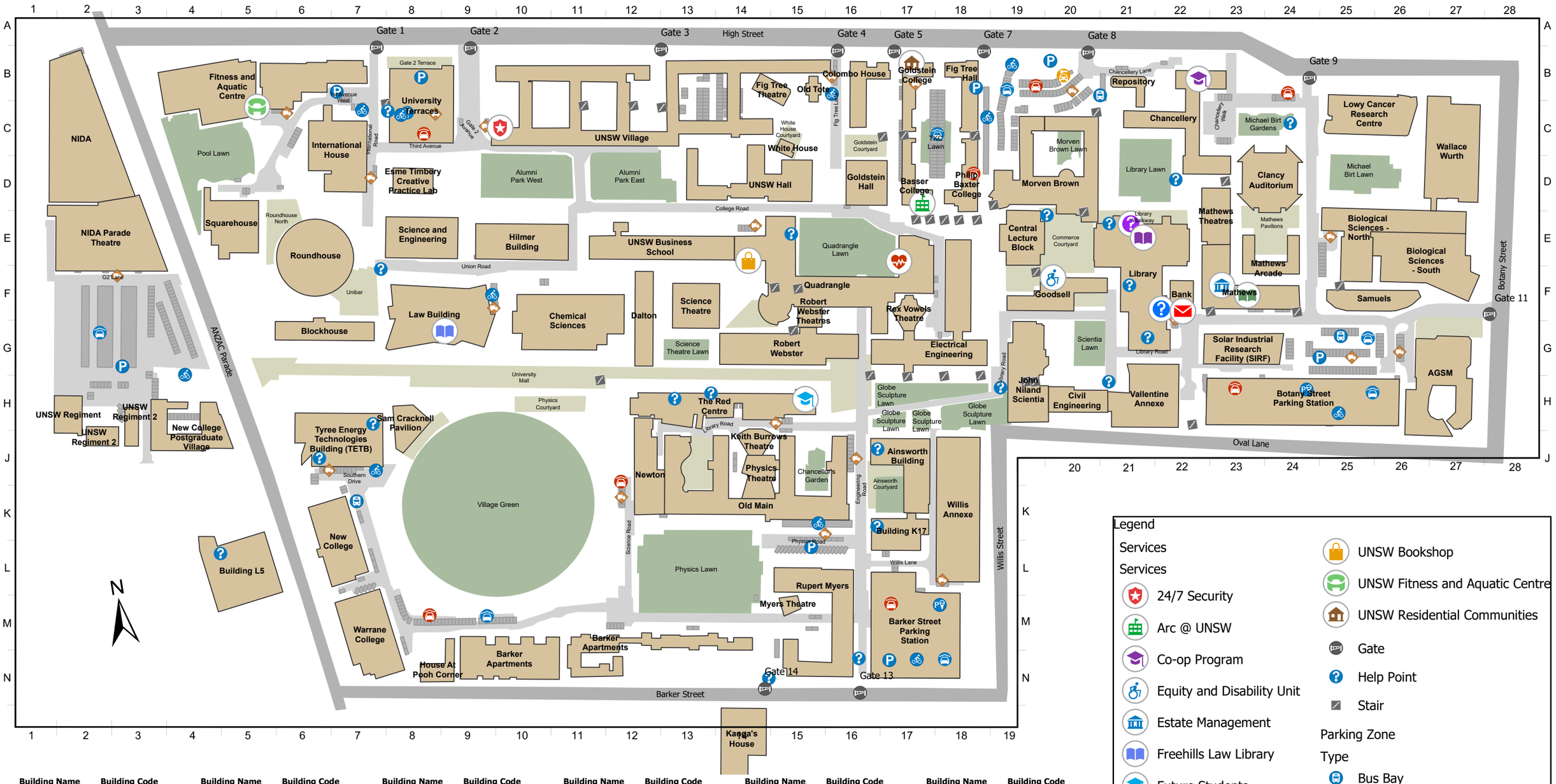

Building Name	Building Code
AGSM	G27
Ainsworth Building	J17
Bank	F22
Barker Apartments	N13
Barker Apartments	N13
Barker Street Parking Station	N18
Basser College	D17
Biological Sciences - North	D26
Biological Sciences - South	E26
Blockhouse	G6
Botany Street Parking Station	H25
Building K17	K17
Building L5	L5

Building Name	Building Code
Central Lecture Block	E19
Chancellery	C22
Chemical Sciences	F10
Civil Engineering	H20
Clancy Auditorium	C24
Colombo House	B16
Dalton	F12
Electrical Engineering	G17
Esme Timbery Creative Practice Lab	D8
Fig Tree Hall	B18
Fig Tree Theatre	B14D
Fitness and Aquatic Centre	B5
Goldstein College	B17

Building Name	Building Code
Goldstein Hall	D16
Goodsell	F20
Hilmer Building	E10
House At Pooh Corner	N8
International House	C6
John Niland Scientia	G19
Kanga's House	O14
Keith Burrows Theatre	J14
Law Building	F8
Library	F21
Lowy Cancer Research Centre	C25
Mathews	F23
Mathews Arcade	E24A

Building Name	Building Code
Mathews Theatres	D23
Morven Brown	C20
Myers Theatre	M15A
New College	L6
New College Postgraduate Village	H3
Newton	J12
NIDA	D2
NIDA Parade Theatre	E2
Old Main	K15
Old Tote	B15
Philip Baxter College	D18
Physics Theatre	K14
Quadrangle	E15

Building Name	Building Code
Repository	B21
Rex Vowels Theatre	F17
Robert Webster	G14
Robert Webster Theatres	G15
Roundhouse	E6
Rupert Myers	M15
Sam Cracknell Pavilion	H8
Samuels	F25
Science and Engineering	E8
Science Theatre	F13
Solar Industrial Research Facility (SIRF)	G23
Squarehouse	E4
The Red Centre	H13

Building Name	Building Code
Tyree Energy Technologies Building (TETB)	H6
University Terraces	B8
UNSW Business School	E12
UNSW Hall	D14
UNSW Regiment	H1
UNSW Regiment 2	J2
UNSW Regiment 2	J2
UNSW Village	B10
Vallentine Annexe	H22
Wallace Wurth	C27
Warrane College	M7
White House	C15
Willis Annexe	J18

Legend

Services

Services

- 24/7 Security
- Arc @ UNSW
- Co-op Program
- Equity and Disability Unit
- Estate Management
- Freehills Law Library
- Future Students
- IT Walk-in Service Centre
- Library
- Medical Centre
- Post Office
- Print Centre
- The Nucleus: Student Hub
- UNSW Bookshop
- UNSW Fitness and Aquatic Centre
- UNSW Residential Communities
- Gate
- Help Point
- Stair

Parking Zone

Type

- Bus Bay
- Accessible
- Go Get
- Loading Zone
- Meter/Permit
- Meters
- Motorbike
- Permit
- Reserve

Date Exported: 31/01/2020 12:22 PM

FLINOVIA PROGRAM

TIME	MON May 22, 2023	TUES May 23, 2023	WED May 24, 2023
8:30	8:30 (30 mins) Arrive/Registration/Coffee	8:30 (30 mins) Arrive/Coffee	8:30 (30 mins) Arrive/Coffee
		Hydroacoustics I: Paul Croaker	**Vibroacoustics II: Cheolung Cheong**
9:00	9:00 (30 mins) Welcome and Opening	9:00 (30 mins) *Noise Emissions from Cavitation Inception During the Interaction of a Pair of Line Vortices: Daniel Knister*	9:00 (30 mins) *Similitude Laws for Scaling Vibrations and Acoustic Radiation of Panels Excited by a Turbulent Boundary Layer: Xavier Plouseau-Guede*
9:30	9:30 (60 mins) Keynote Aeroacoustic noise produced by small unmanned aerial vehicle propellers: Michael Kingan, University of Auckland	9:30 (30 mins) *Study of Flow Noise with a Buoyancy-Driven Model: Ian MacGillivray*	9:30 (30 mins) *Acoustic Measurements of Multiphase Tip-Leakage Flow: Patrick Russell*
10:00		10:00 (30 mins) *Hydroacoustic and FSI development of the AMC water tunnel: Paul Brandner*	10:00 (30 mins) *Reduced-order modelling of flow-induced vibration from turbulence impingement: Kostas Tsigklifis*
10:30	10:30 (30 mins) Morning Tea Break	10:30 (30 mins) Morning Tea Break	10:30 (30 mins) Morning Tea Break
	Wall Pressure I Chair: Carsten Spehr	**Computational Modelling I Chair: Mahmoud Karimi**	**Wall Pressure II Chair: Xin Zhang**
11:00	11:00 (30 mins) *Noise induced from near-axial flow in a cylindrical towed model: Jan Abshagen*	11:00 (30 mins) *Broadband noise predictions using large eddy simulations: further analysis of boundary layer statistics: Johan Bosschers*	11:00 (30 mins) *Calculating uncertainty of flow-induced vibration simulations: Stephen Hambric (Hybrid)*
11:30	11:30 (30 mins) *Efficient Large-Eddy Simulation Methods for Predicting Wall-Pressure Fluctuations Beneath a Turbulent Boundary Layer: Graeme Lane*	11:30 (30 mins) *Mitigation of Cavity Noise with Aeroacoustically Excited Surface Panels: Muhammad Naseer*	11:30 (30 mins) *Wavenumber spectrum determination for transsonic wind tunnel measurements using FISTA: Carsten Spehr*
12:00	12:00 (30 mins) *Amiet's theory for wall-pressure fluctuations on an airfoil in turbulence: Fernanda dos Santos*	12:00 (30 mins) *Aeroacoustic source contribution to sound power for jet flows: Esmaeel Eftekarian*	12:00 (30 mins) *Measurements of wavenumber-frequency spectra in an open-jet pressure gradient facility: Chaoyang Jiang*
12:30	12:30 (90 mins) Lunch Break	12:30 (90 mins) Lunch Break	12:30 (90 mins) Lunch Break
13:00			
13:30			
	Aeroacoustics I Chair: Hiroshi Yokoyama	**Aeroacoustics II Chair: Elias Arcondoulis**	**Aeroacoustics III: Danielle Moreau**
14:00	14:00 (30 mins) *A review of structured porous materials in aeroacoustics: what we know and where to next: Elias Arcondoulis*	14:00 (30 mins) *Porous edges for flow noise reduction: from theory to application: John Kershner*	14:00 (30 mins) *Fluid-acoustic interactions with resonance around an axial fan in a duct: Hiroshi Yokoyama*
14:30	14:30 (30 mins) *Transient aeroacoustic analysis of low Reynolds number pitching foil and the effect of surface treatment: Xin Zhang*	14:30 (30 mins) *Modelling complex turbulence: Alistair Hales*	14:30 (30 mins) *Acoustic Waves in a Planar Supersonic Wake: Manuj Awasthi*
15:00	15:00 (30 mins) *Data-driven symbolic regression for the modelling of correlation functions of wall pressure fluctuations under turbulent boundary layers: Alessandro Casaburo (Hybrid)*	15:00 (30 mins) *Modelling and characterization of micro-porous resonating liners under a low speed flow: Cedric Maury (Hybrid)*	15:00 (30 mins) *Acoustic metaliner for sound insulation in a duct with flow: Wonju Jeon*
15:30	15:30 (30 mins) Afternoon Tea Break	15:30 (30 mins) Afternoon Tea Break	15:30 (30 mins) Farewell Afternoon Tea
	Vibroacoustics I Chair: Paul Dylejko		
16:00	16:00 (30 mins) *High-fidelity Prediction of Vehicle Indoor Noise due to External Flow Disturbances: Cheolung Cheong*	16:00 (30 mins) Defence Science and Technology Group Invited Presentation	16:00 (60 mins) Flow Noise Group Lab Tour
16:30	16:30 (30 mins) *Acoustic source localisation from vibration measurement of a plate beneath a turbulent boundary layer: Mahmoud Karimi*	Dr Greg Bain, Acting Chief Platforms, Defence Science and Technology Group	(covered shoes required)
17:00	17:00 (30 mins) *Investigations about the experimental application of PEDEm for the reproduction of a structural response to a Turbulent Boundary Layer excitation: Guilia Mazzeo*	Speakers to make way to dinner venue: Cafe Sydney, 5th Floor, Customs House 31 Alfred Street, Circular Quay, NSW, 2000	
17:30			
18:00			
		19:30 Speaker Dinner (Cafe Sydney)	

FLINOVIA IV Abstracts

Noise induced from near-axial flow in a cylindrical towed model

Jan Abshagen[1]

[1]Bundeswehr Technical Center for Ships and Naval Weapons, Maritime Technology and Research (WTD 71)
Berliner Straße 115, 24340 Eckernförde, Germany
e-mail: janabshagen@bundeswehr.org

Linear hydroacoustic antennas towed behind a platform, so-called *towed arrays* or *acoustic streamers*, are predominately utilized for underwater detection and seismic exploration at sea. In general such a hydroacoustic receiving system consists of a flexible (cylindrical) tube with a radius of a few centimeters and a length ranging from a few meters up to several hundred meters or even a few kilometers. For stationary towing conditions, i.e. constant towing speed and depth, the turbulent boundary layer that forms around the cylindrical outer hull can be approximately considered as axisymmetric. An axisymmetric turbulent boundary layer has different properties, for instance the boundary layer thickness, if compared to flat plate conditions (see, e.g., [1]). Wall pressure fluctuations beneath the (outer) axisymmetric turbulent boundary layer excite the elastic hull and the resulting hydroacoustic noise in the quiescent interior of the antenna interferes the reception of (far-field) underwater sound at the hydrophones. At typical towing speeds from a few meters per second and a sufficient distance from the towing vessel the interior noise, that stem from the turbulent boundary layer on the outer hull, is the predominant contribution to the so-called sonar self-noise and limits the performance of a sonar system [2].

The properties of turbulent wall pressure fluctuations are substantially altered in the presence of flow disturbances, such as surface inhomogeneities on the elastic hull of an underwater receiving system [3]. This can have substantial influence on the generation of flow induced interior noise [4]. For a towed array, an example of a geometric flow disturbance arises from a local cross-sectional enlargement which can lead to separation (and reattachment) of the axisymmetric turbulent boundary layer [5]. Boundary layer properties can, however, also be altered in the case of homogeneous surfaces if the inflow is asymmetric. Near-axial inflow on cylindrical structures, for instance, can lead to vortex shedding [6].

In this work we have studied the generation of interior noise induced from turbulent boundary layer flows in a cylindrical model section that in embedded in a long towed array. The towing experiments were performed with RV PLANET under deep water conditions at different towing speeds. Flow noise measurements are conducted with an array of hydrophones and noise separation methods are applied in order to extract the flow induced pressure fluctuations from the acoustical far-field noise. Particular focus is given to the influence of near-axial inflow conditions, that arises during course changes of the vessel, on the properties on the interior flow noise.

References

[1] F. Wachter, A. Metelkin, J. Jovanovic, J. Praß, and S. Becker, "Numerical investigation of the effect of convex transverse curvature and concave grooves on the turbulent boundary layer along a cylinder in axial flow," *International Journal of Heat and Fluid Flow*, vol. 92, p. 108855, 2021.

[2] R. Urick, *Principles of Underwater Sound.* New York: McGraw-Hill, 2nd ed., 1975.

[3] J. Abshagen and V. Nejedl, "Underwater flow noise from a turbulent boundary layer over a wavy surface," in *Flinovia - Flow Induced Noise and Vibration Issues and Aspects - III* (E. Ciappi, S. de Rosa, F. Franco, J.-L. Guyader, and S. Hambric, eds.), Springer, Cham, 2021.

[4] J. Abshagen, "Interior noise from a flow past an obstacle in an underwater experiment," in *Proc. 48th Annual German Conference on Acoustics (DAGA 2022)*, pp. 720–722, German Acoustical Society (DEGA), 2022.

[5] J. Abshagen and V. Nejedl, "Noise induced in a cylindrical towed model from separated/reattached turbulent flow," in *INTER-NOISE and NOISE-CON Congress and Conference Proceedings, NOVEM 2018, Ibiza, SPAIN*, pp. 587–596(10), Institute of Noise Control Engineering, 2018.

[6] M. Bull and W. Dekkers, "Vortex shedding from long slender cylinders in near-axial flow," *Phys. Fluids A*, vol. 5, no. 12, pp. 3296–3298, 1993.

A review of structured porous materials in aeroacoustics: what we know and where to next

Elias Arcondoulis[1]

[1]Lecturer in Aerospace Engineering, University of Bristol, BS8 1TR, U.K.

Email: elias.arcondoulis@bristol.ac.uk

Open cell porous media, such as metal foam and porous polyurethane have been fitted to both bluff and aerodynamic bodies, for the purpose of passive flow and noise control. Applications in the field of aeroacoustics include porous coated cylinders, porous leading and trailing edges of airfoils, slate coves of wings and coatings of high-speed train pantographs. To understand how these unstructured porous media reduce flow induced noise and control the wake region, the internal flow field within the porous media requires investigation. Until recently, the fundamental flow dynamics within the porous layer was restricted to numerical simulations that involved assuming that the porous media possessed bulk averaged properties, with constant porous parameters (porosity, pores per inch, permeability). Typically, these assumptions model the internal flow field sufficiently to accurately model external flow fields (i.e., the flow within the porous media generates accurate flow fields outside the porous media such as the wake) yet the fundamental flow mechanisms within the porous media responsible for passive flow and noise control cannot be ascertained from these approximations. Experimental investigations of unstructured porous media internal flow fields are extremely difficult to conduct due to lack of line of sight within the material for experimental techniques such as particle image velocimetry (PIV) and constant temperature hot-wire anemometry.

To investigate the internal flow field of porous media, Arcondoulis et al. [1] developed a type of structured porous media via self-repeating structures such as intersecting C-shapes in orthogonal directions. By modifying the intersecting geometry, porous media with specific porosity, pores per inch and permeability can be easily manufactured. In addition, these designs can be 3-D printed using transparent media, which opens up the use of index refracting matching (IRM) and tomographic PIV. Furthermore, their self-repeating structure allows 2-D numerical simulations to be conducted to simulate a slice of the internal flow field. To date, structured porous media have been applied to airfoil leading and trailing edges, cylinders in uniform flow and appended to the blunt trailing edge of a plate. Their aeroacoustic performance typically matches that of unstructured porous media with the same porous properties. This key result implies that the internal flow field of unstructured porous media can be understood by investigating the internal flow field of structured porous media, which is possible both numerically and experimentally. This provides a key step in developing optimized porous media for passive flow and noise control.

In this paper, a review of structured porous media will be presented, covering published numerical and experimental results to date, and in some cases their performance will be compared against unstructured porous media. Some potential future applications will also be discussed that extend beyond the field of aeroacoustics into civil and coastal engineering applications.

References

[1] Arcondoulis, E.J.G, Liu, Y., Li, Z., Yang, Y. and Wang, Y., 2019. “Structured porous material design for passive flow and noise control of cylinders in uniform flow”, *Materials*, vol. 12, no. 18, p.2905.

Acoustic Waves in a Planar Supersonic Wake

Manuj Awasthi [1*], Sean McCreton[1] Danielle Moreau [1] Con Doolan

[1] Flow Noise Group, School of Mechanical and Manufacturing Engineering,

UNSW, Sydney 2052, Australia

* Email: m.awasthi@unsw.edu.au

Acoustic waves in supersonic flows play an important role, as they can set up resonant processes that not only cause annoyance but also introduce significant surface pressure loading, which can affect the performance of aero engines such as scramjets. While extensive work has been done on the aeroacoustics of high-speed jets due to the screech problem [1], relatively little is known about the behaviour of acoustic waves in supersonic wake flows. Recent work on supersonic wake of a circular cylinder [2, 3] has shown that the acoustic waves in the near wake could be responsible for setting up vortex shedding in the wake with a characteristic frequency that is nearly twice that of the canonical incompressible cylinder wake. The present work attempts to understand the role acoustic waves play in a Mach 3 planar supersonic wake by visualizing the flow behind a two-dimensional circular cylinder using high-speed visualization techniques. The wake was visualized using a high-speed focusing schlieren system to suppress the effects of density gradients within the side-wall boundary layers and reveal the disturbance field within the two-dimensional region of interest.

Figure 1 below shows the instantaneous flow-field behind the circular cylinder as visualized using the schlieren system. The light intensity in the image is proportional to the streamwise density gradient in the flow-field since a vertical knife-edge was utilised. The location of the cylinder and the salient features of the flow-field extracted from [3] have been overlaid on the image for spatial reference. The schlieren dataset is both spatially and temporally resolved (up to 50 kHz) and it will be analysed through spectral proper orthogonal decomposition (SPOD) method to yield orthogonal spatial modes that oscillate at a given frequency. Figure 2 below shows one such spatial mode at a Strouhal number (St_d) of 0.03. The mode clearly shows a large-scale organised motion in the wake with the disturbances in the shear layers, the reattachment region and the recompression shocks oscillating in-phase (same-sign SPOD eigenvector). There is also an out-of-phase disturbance overriding the shear layers which could be related to the acoustic waves observed in the instantaneous image in Figure 1. Lastly, the SPOD mode also shows large-scale disturbances in the near wake that extend beyond the mean wake boundary and appear to merge with the recompression waves. Similar disturbances are also visible in the instantaneous image, and it is possible that these structures represent acoustic disturbances that originate from the recompression waves.

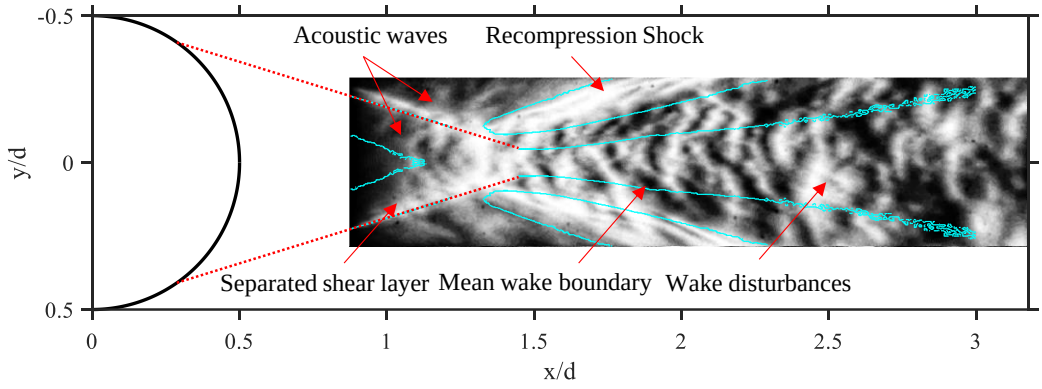

Figure 1 Instantaneous flow-field behind a circular cylinder placed in Mach 3 flow.

The high-speed schlieren images of the cylinder wake will be further analysed using SPOD modes at different frequencies and other spatio-temporal data reduction methods (e.g., bandpass-filtered images, wavenumber-frequency spectrum). The emphasis of this analysis will be on revealing the nature

of the acoustic waves in the cylinder wake and how these waves interact with the recompression shocks and wake turbulence.

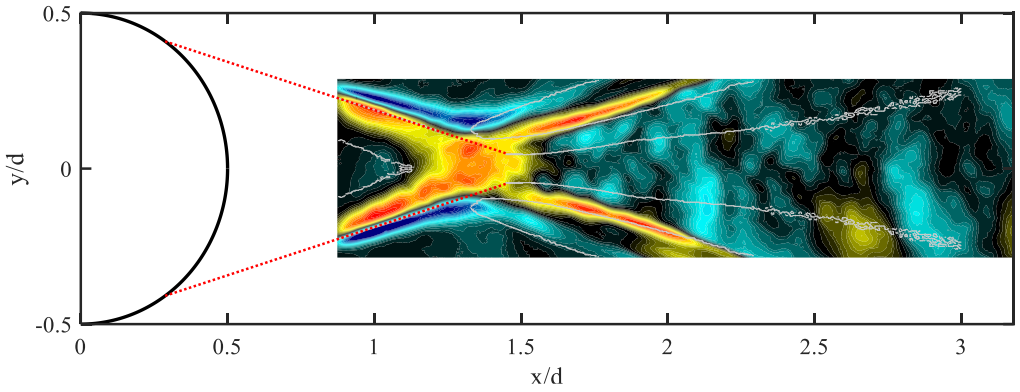

Figure 2 Most energetic SPOD mode of the schlieren wake dataset at $St_d = 0.03$

References

[1] D. Edgington-Mitchell, T. Wang, P. Nogueira, O. Schmidt, V. Jaunet, D. Duke, P. Jordan, A. Towne, "Waves in screeching jets," *Journal of Fluid Mechanics*, vol. 913, 2021.

[2] Schmidt, B. E. & Shepherd, J. E. "Oscillations in cylinder wakes at Mach 4," *Journal of Fluid Mechanics* vol. 785, 2015.

[3] M. Awasthi, S. McCreton, D.J. Moreau, C.J. Doolan, "Supersonic cylinder wake dynamics," *Journal of Fluid Mechanics*, vol. 945 (2022).

Modelling complex turbulence

Lorna J Ayton[1] and Alistair D G Hales[1]

[1]Department of Applied Mathematics and Theoretical Physics, University of Cambridge, Wilberforce Road, CB3 0WA, UK
e-mail: lja30@cam.ac.uk

Aeroacoustic noise is generated by the interaction of turbulent flow with structures placed within the flow. The turbulence could be generated elsewhere, i.e. upstream of the structure of interest, or by the structure itself and lie within a turbulent boundary layer. In either case, the typical approach from a theoretical modelling viewpoint is to decompose the turbulence into a series of Fourier components (often called 'gusts'), and solve the Linearised Euler Equations for the noise generated by one component. The noise due to fully turbulent flow is then recovered by 'adding together' the individual Fourier components which make up the true turbulence. Of course, in the continuum of turbulence, this 'adding' is in fact an integral over a turbulent spectrum which describes the structure of the turbulence.

Mathematically, we prescribe the turbulence via potential or pressure fluctuations, $\phi^{(I)}$, as

$$\phi^{(I)} = \int_{-\infty}^{\infty}\int_{-\infty}^{\infty} w_2(\mathbf{k}) e^{i\mathbf{k}\cdot\mathbf{x}-i\omega t}\mathrm{d}k_2\mathrm{d}k_3$$

where we assume the turbulence convects at speed $k_1 = \omega/U$, where U is a given streamwise velocity. Supposing the acoustic pressure response due to one component, $we^{i\mathbf{k}\cdot\mathbf{x}-i\omega t}$, is given by

$$p_s(\boldsymbol{k},\omega) = wP(\boldsymbol{k},\omega)$$

then the total scattered noise due to all turbulence is given by

$$p_t(\omega) = \int_{-\infty}^{\infty}\int_{-\infty}^{\infty}\int_{-\infty}^{\infty} w_2(\mathbf{k})P(\mathbf{k},\omega)\delta\left(k_1 - \frac{\omega}{U_\infty}\right)\mathrm{d}k_1\mathrm{d}k_2\mathrm{d}k_3$$

By defining

$$\Pi(\mathbf{k}) = \lim_{T\to\infty}\frac{\pi}{T} w_2(\mathbf{k})w_2^*(\mathbf{k}),$$

the total sound power spectral density is given by

$$\Psi(\omega,\theta) = \int_{-\infty}^{\infty}\int_{-\infty}^{\infty}\int_{-\infty}^{\infty} |P(\mathbf{k})|^2\Pi(\mathbf{k})\delta\left(k_1 - \frac{\omega}{U}\right)\mathrm{d}k_1\mathrm{d}k_2\mathrm{d}k_3, \tag{1}$$

where δ is the Dirac delta function encapsulating the expected convection speed of the turbulence.

It is well established that the single-component solution for the interaction of a gust with a flat plate aerofoil (either at the leading edge, or the trailing edge), with or without serrations, or with elements of poroelasticity, can be determined typically through the Wiener Hopf method. Finite plate effects, and the effects of thickness can also be included. One would then hope that theoretical predictions and experimental measurements are consistent, however, in the case of complex turbulence, an insufficient understanding of Π means the model becomes one of garbage in garbage out.

This can be particularly problematic in the case of trailing-edge bio-inspired adaptations, where alterations to the surface itself not only modify the scattering, but modify the generation of the turbulence itself.

When one supposes homogeneous isotropic turbulence, for which there are a multitude of empirical models, experimentally this can be very difficult to generate precisely, therefore some effects of anisotropy can contaminate the measurements [1]. We thus seek a way to develop more accurate turbulence models which can be applied to a variety of aeroacoustic scattering situations.

We therefore need a way to calculate $\Pi(\boldsymbol{k})$ accurately and efficiently. For leading-edge noise (i.e. upstream turbulence, where $\Pi = \Phi_{22}$ is common notation) we do so via Gaussian decomposition. We seek a function, f, for which

$$\Phi_{22}(\mathbf{k}) = \int_0^\infty f(l)\Phi_{22}^{a,G}(\mathbf{k})\mathrm{d}l, \tag{2}$$

where

$$\Phi_{22}^{a,G}(\mathbf{k}) = \frac{u^2 u_r^2 l^5 \Lambda_r (k_1^2 + k_3^2)}{\pi^4} \exp\left(-\frac{l^2(k_1^2 + \Lambda_r^2 k_2^2 + k_3^2)}{\pi}\right). \tag{3}$$

is a standard Gaussian spectrum with a ratio of Λ_r between axial and radial turbulence lengthscales ($\neq 1$ in the case of anisotropy). We discretise the integral to

$$\overline{\Phi_{22}}(\mathbf{k}) = \sum_{m=0}^{M} \frac{\hat{f}(l_m)\Delta l_m}{\sum_{m=0}^{M} \hat{f}(l_m)\Delta l_m} \Phi_{22}^{a,G}(\mathbf{k}; l_m)$$

The nature of the Gaussian decomposition means that the energy spectrum also satisfies

$$E^a(\kappa) = \sum_{m=0}^{M} \frac{\hat{f}(l_m)\Delta l_m}{\sum_{m=0}^{M} \hat{f}(l_m)\Delta l_m} E^{a,G}(\kappa; l_m).$$

thus we could recover f, via the Gaussian transform [2], and the required weightings, from measurements of the one-dimensional function, E, rather than detailed measurements of a multi-dimensional function Φ_{22}.

We illustrate the comparison of the Gaussian decomposition versus experimental data for the SPL of anisotropic turbulence in Figure 1.

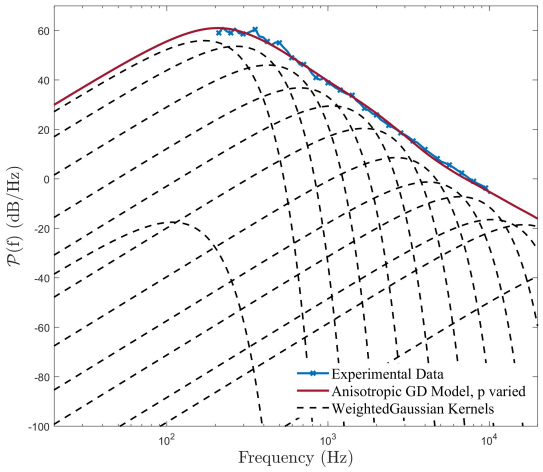

Figure 1: Comparison of GD and experimental measurements for SPL alongside the weighted kernels being summed.

For trailing-edge noise (i.e. boundary layer turbulence) the TNO model is commonplace, however assumes a rigid impermeable flat surface. For bio-inspired adaptations, a surface could be porous and/or elastic leading to a required alteration of the model, the derivation of which will be presented.

References

[1] H. A. Abid, A. P. Markesteijn, S. A. Karabasov, B. Zang, M. Azarpeyvand, and Y. D. Mayer, "Improving accuracy of airfoil trailing edge noise models with turbulent flow anisotropy," in *28th AIAA/CEAS Aeroacoustics 2022 Conference*, p. 3105, 2022.

[2] A. M. Wohlbrandt, N. Hu, S. Guérin, and R. Ewert, "Analytical reconstruction of isotropic turbulence spectra based on the gaussian transform," *Computers & Fluids*, vol. 132, pp. 46–50, 2016.

Data-driven symbolic regression for the modelling of correlation functions of wall pressure fluctuations under turbulent boundary layers

A. Casaburo[1,2], G. Petrone[2,3], E. Ciappi[4], F. Franco[2,3], and S. De Rosa[2,3]

[1]Laboratoire de Tribologie et Dynamique des Systèmes (LTDS), École Centrale de Lyon, 36 Av. Guy de Collongue, 69134 Écully, France
Email: alessandro.casaburo@ec-lyon.fr
[2]WaveSet S.R.L., Via A. Gramsci 15, 80122, Naples, Italy
[3]pasta-Lab, Dipartimento di Ingegneria Industriale, Sezione Aerospaziale, Università degli Studi di Napoli Federico II, Via Claudio 21, 80125 Naples, Italy
Email: giuseppe.petrone@unina.it
Email: francof@unina.it
Email: derosa@unina.it
[4]CNR-INM, Via di Vallerano 139, 00128 Rome, Italy
Email: elena.ciappi@cnr.it

The Turbulent Boundary Layer (TBL) is an important source of noise and vibrations in transport engineering (aerospace, automotive, naval, railway), whose consequences must not be underestimated. On the one hand, induced vibrations in the interior of the vehicle can exceed the design requirements and cause damages to the payload. On the other hand, vibrations of the exterior can degenerate and lead to fatigue or, in the worst case, structural damage. Last, but not least, wall-pressure fluctuations (WPFs) associated with the turbulence can significantly excite a structure which, in turn, radiates acoustic power. Consequently, this stochastic pressure, random in both time and space domains, is one of the main sources of air-borne noise that, along with the structural-borne sound generated by the vehicle disturbing the flow, can produce discomfort to passengers, pilots, and the surrounding environment. It is, therefore, clear that a good description of the WPFs is required to accurately predict the propagation of noise and the induced vibrations. Mathematical models of TBL excitation take the form of statistical space-time correlation functions and their corresponding wavevector-frequency spectra; broadly speaking, these models can be split into two contributions: single-point wall-pressure spectrum and correlation function. The former is representative of the distribution of the mean-square fluctuating pressure in frequency, therefore it acts as an amplitude term useful to estimate the amount of energy involved in the phenomenon. The latter describes the spatial correlation of the pressure field and, therefore, how the information of the disturbance spreads in the spatial domain. Many models are present in literature [1]; all of them are semi- or fully empirical and their derivation can be considered somewhat *ad hoc*, even though rooted in the physics of the boundary layer. The direct consequences are that these models describe quite well the dataset on which they are based, but seldom provide a satisfactory agreement over the complete range of available data. Their prediction capability is limited to particular frequency and wavenumber ranges, and usually require the calibration of several coefficients to match amplitudes and transition frequencies between the several frequency regimes

observed during the experiments [2]. Moreover, other issues (e.g. integration scheme, frequency range) must be considered when numerical simulations are performed, since the transformation of the pressure distribution into discrete locations is a delicate phase affecting both the accuracy and computational time [3]. Some of these problems are addressed by modifications of existing models [4, 5], but only partially. The idea underpinning this work is to exploit the increasing number of experimental data, along with the exponential improvement of data-driven techniques, to give new lifeblood to the derivation of WPFs models. In particular, the potentialities of symbolic regression through Gene Expression Programming (GEP) are investigated to derive new empirical models that are not based on already existing ones but are estimated by training the algorithm on experimental data. Once the best models are selected, a direct comparison, in terms of mathematical form and predictive capabilities, is made with some consolidated literature models to establish whether there is an actual improvement in estimating the correlation function.

References

[1] T. S. Miller, J. M. Gallman, and M. J. Moeller, "Review of turbulent boundary-layer models for acoustic analysis", *Journal of Aircraft*, vol. 49, no. 6, pp. 1739-1754, 2012
[2] M. K. Bull, "Wall-pressure fluctuations beneath turbulent boundary layers: some reflections on forty years of research", *Journal of Sound and Vibration*, vol. 190, no.3, pp. 299-315, 1996
[3] F. Franco, S. De Rosa, E. Ciappi, "Numerical approximations on the predictive responses of plates under stochastic and convective loads", *Journal of Fluids and Structures*, vol. 42, pp. 296-312, 2013
[4] S. Finnveden, F. Birgersson, U. Ross, T. Kremer, "A model of wall pressure corelation for prediction of turbulence-induced vibration", *Journal of Fluids and Structures*, vol. 20, pp. 1127-1143, 2005
[5] A. Caiazzo, R. D'Amico, W. Desmet, "A Generalized Corcos model for modelling turbulent boundary layer wall pressure fluctuations", *Journal of Sound and Vibration*, vol. 372, pp.192-210, 2016

Transient aeroacoustic analysis of low Reynolds number pitching foil and the effect of surface treatment

Wangqiao Chen[1], Siyang Zhong[2], Peng Zhou[1], and Xin Zhang[1]

[1]Department of Mechanical and Aerospace Engineering, Hong Kong University of Science and Technology
Clear Water Bay, Kowloon, Hong Kong SAR, China
e-mail: aexzhang@ust.hk
[2]Department of Aeronautical and Aviation Engineering, The Hong Kong Polytechnic University
Hung Hum, Kowloon, Hong Kong SAR, China

Abstract

This work experimentally investigates the aeroacoustics of a small-scale airfoil under high-rate pitching motion in an anechoic wind tunnel. The wind speed ranges from $10\,\mathrm{m/s}$ to $40\,\mathrm{m/s}$, and the chord-length based Reynolds number ranges from 3.2×10^4 to 1.3×10^5. The acoustic measurements show that the trailing edge noise from a pitching airfoil occurs around zero angle of attack during each pitching process. A wavelet-based beamforming method is employed to image the noise sources in the time-frequency domain. The transient flow field is measured using the particle image velocimetry. The results show that tonal noise at different frequencies can be generated due to the vortex shedding from the trailing edge. The leading edge separation interacts with the trailing edge and induces broadband noise with a varying central frequency. The transient noise generation process is discovered by synchronizing acoustic and fluid measurements.

The urban aerial mobility (UAM) rotor noise with vertical disturbances is a practical problem but has not yet received much attention. The velocity of the vertical disturbance in an urban environment can modify the inflow conditions, resulting in dramatic periodic variations in the relative angle of attack of the blades. The complex inflow conditions make it challenging to study the rotor noise in vertical disturbance by rotor experiments. In this work, we employ a 2-D simplified model, which assumes the vertical disturbance effects on the UAM rotor as a high-rate pitching motion, to understand the fundamental aeroacoustic mechanisms.

Vortex structures generated at leading edge and trailing edge of the pitching flat plate are important transient flow features [1, 2]. Granlund et al. [1] show that the leading edge vortex was formed at high pitch rates by using a qualitative flow visualization method. Baik et al. [2] concluded that the leading-edge vortex circulation increased linearly with the motion phase, and its size follows a power law at low Reynolds number (from $O(10^3)$ to $O(10^4)$). They also proposed that the reduced frequency is the main parameter, which affects the growth rate of the leading-edge vortex and delays the formation and shedding of the trailing edge vortex. Jantzen et al. [3] studied the effect from the tip vortex by using the three-dimensional direct numerical simulations. The transient flow field and corresponding aerodynamic coefficients constitute the key contribution of these studies.

The transient flow field is related to the noise generation process. Typically, the leading edge vortex interaction and separation on the wing surface at high pitch rates would significantly affect the flow field around the trailing edge [2], and the far-field trailing edge noise should also be influenced accordingly. To analyze the acoustic signature of the transient sources, a phase-averaged wavelet-based beamforming method [4] will be employed in this work to capture the sound source in the time-frequency domain with a high resolution. Particle image velocimetry (PIV) method will be combined with the acoustic measurements to reveal the transient flow field during the pitching process.

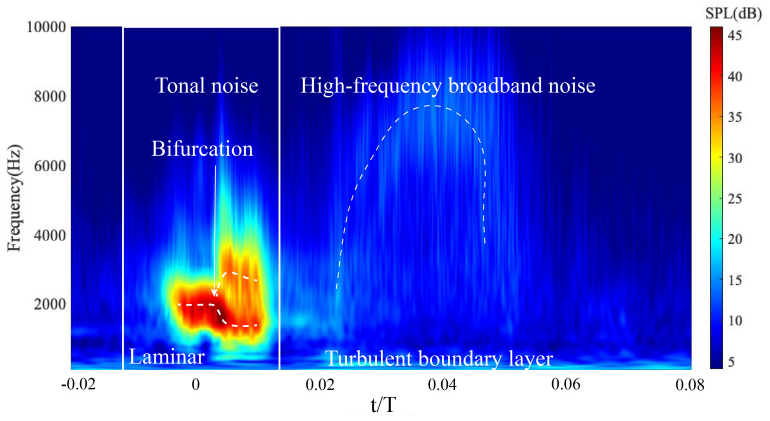

Figure 1: Phase-averaged time-frequency spectrum results of pitching wing noise at 20 m/s.

Figure 1 shows the phase-averaged time-frequency spectrum results of pitching airfoil noise at 20 m/s. Here $T = 2.5$ s is the pitching period. The waveform of the pitching process will be shown in full length article. Airfoil boundary layer varies from laminar to turbulence periodically. The solid lines separate the laminar and turbulent boundary layer regions and the dashed line denotes the varying process of the centre frequency of pitching airfoil noise. The airfoil achieves zero angle of attack at $t/T = 0$. The zero angle of attack location is verified by the stable airfoil and force measurement systems. First, the tonal noise is generated by the vortex shedding process around the zero angle of attack. Then, around $0.008\,T$, the periodic fluctuations in the laminar boundary layer are obvious and produce the tonal noise at a higher frequency. The tonal frequency splits into two different frequencies, thus creating a bifurcation in Fig. 1. Next, the laminar boundary layer transits to a turbulence boundary layer at $0.016\,T$ and the tonal noise disappears.

The tonal noise generation process can be understand by following classical trailing edge noise theories. However, the high-frequency broadband noise, as shown in Fig. 1 is much more complex. The flow structures separated from the leading edge interacts with the airfoil trailing edge, and produce the high-frequency broadband noise as shown in Fig. 1. The details of flow fields, noise sources acoustic imaging results, and analysis at other inflow conditions will be shown in full length article.

References

[1] K. Granlund, M. Ol, and L. Bernal, "Unsteady pitching flat plates," *Journal of Fluid Mechanics*, vol. 733, p. R5, 2013.

[2] Y. S. Baik, L. P. Bernal, K. Granlund, and M. V. Ol, "Unsteady force generation and vortex dynamics of pitching and plunging aerofoils," *Journal of Fluid Mechanics*, vol. 709, p. 37–68, 2012.

[3] R. Jantzen, K. Talra, K. Granlund, and M. Ol, "Vortex dynamics around pitching plates," *Physics of Fluids*, vol. 26, p. 053606, 2014.

[4] W. Chen and X. Huang, "Wavelet-based beamforming for high-speed rotating acoustic source," *IEEE Access*, vol. 6, pp. 10231–10239, 2018.

High-fidelity Prediction of Vehicle Indoor Noise due to External Flow Disturbances

Songjune Lee[1] and Cheolung Cheong[2]

[1]Jeju Global Research Center, Korea Institute for Energy Research
Haemajihaeanro 200, Gujaub, Jeju 63357, Rep. of Korea
Email: sjlee83@kier.re.kr
[2]School of Mechanical Engineering, Pusan National University
2, Busandaehak-ro 63beon-gil, Geumjeong-gu, Busan, 46241, Rep. of KOREA
Email: cheong@pusan.ac.kr

A pleasant and quiet car cabin is one of the most critical factors affecting customers' choices in the vehicle market. As the traditional noise sources, such as the power train, become less, the relative contribution of aerodynamic noise to the interior noise of a road vehicle becomes even more critical. The physical process of the interior transmission of external flow disturbances can be understood by three sequential mechanisms: external flow excitation of vehicle window shields, the vibrational response of the windshields to the external flow disturbances, and the acoustic response of a cabin room to the windshield vibration. A reliable numerical method suitable for each phase needs to be developed and combined for a high-fidelity prediction of the indoor noise due to external flow. In this study, a high-fidelity numerical methodology was developed for the reliable prediction and analysis of the interior transmitted noise due to external flow disturbances. The developed numerical methods were based on the sequential application of the high-resolution LES technique, the wavenumber-frequency transform, and the vibroacoustic model.

Figure 1 shows the overall application procedure of the flow-vibroacoustic model developed in this study. The developed methods were applied to the benchmark problem of the Hyundai-Simplified Model (HSM) [1]. First, the compressible LES techniques with high-resolution grids were employed to accurately predict the external turbulent flow and aeroacoustic fields due to the turbulent flow, at the same time, of the HSM in an anechoic wind tunnel at a flow speed of 110 km/h. The validity of the flow simulation result was confirmed by comparing the predicted surface pressure spectrum with the measured ones. Second, surface pressure fluctuations on the front windshield and side windows, which were obtained from the LES simulation, were decomposed into incompressible and compressible ones using the wavenumber-frequency analysis. The former was associated with convected turbulence fluctuation, and the latter was related to acoustic waves. Lastly, the interior sound pressure levels were predicted using the vibroacoustic solver for the vehicle cabin, which solved the one-way fluid/structure-acoustic interaction problem with the input of the incompressible and compressible pressure fields. Especially the injected power formula was employed to account for the vibration characteristics of the structure and thus to improve the accuracy of the vibroacoustic solver [2]. The prediction results showed excellent agreement with the measured data. In addition, it was found that the compressible pressure field dominantly contributed to the interior noise in a wide high-frequency range. This result revealed that, although the magnitudes of the compressible pressure

components were generally lower than those of the incompressible ones, their contribution to the interior noise was more dominant because the speed of compressible waves, i.e., the speed of sound is much higher than that of the incompressible pressure comparable to the vehicle cruising speed. Therefore, it is the first measure for a quiet cabin to reduce external aerodynamic noise.

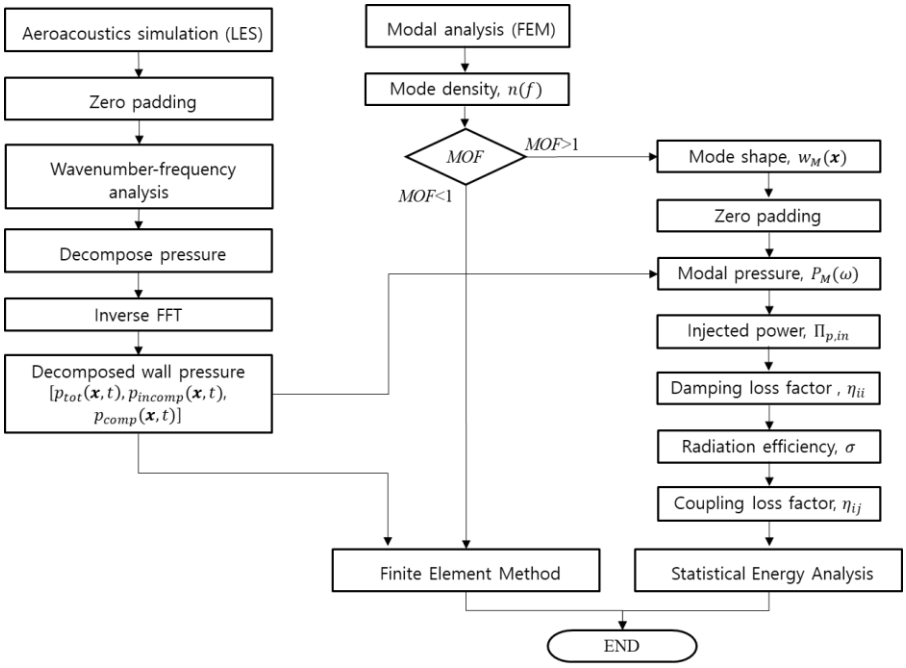

Figure 1: Workflow of developed flow-vibroacoustic solver

References

[1] M. Cho, H. Kim, C. Oh, K. Ih, A. Khondge, F. Mendonca, J. Li, E. Choi, B. Ganty, and R. Halles, “Benchmark study of numerical solves for the prediction of interior noise transmission excited by A-pillar vortex,” *Inter-noise 2014*, Melbourne, Australia, 2014.

[2] S. Lee, S-h. Lee, and C. Cheong, “Development of High-Fidelity Numerical Methodology for Prediction of Vehicle Interior Noise Due to External Flow Disturbances Using LES and Vibroacoustic Techniques," *Applied Sciences*, vol. 12, no. 13, pp. 1-25, 2022.

Amiet's theory for wall-pressure fluctuations on an airfoil in turbulence

Fernanda L. dos Santos[1,*], L. Botero-Bolívar[1], Christ A.F. de Jong[2], Roel A.J. Müller[2], Johan Bosschers[3], Cornelius H. Venner[1], and Leandro D. de Santana[1]

[1]Engineering Fluid Dynamics group, University of Twente, 7500 AE, Enschede, The Netherlands
[2]Acoustics and Sonar, TNO, 2597 AK, The Hague, The Netherlands
[3]Maritime Research Institute Netherlands (MARIN), 6708 PM, Wageningen, The Netherlands
[*]Corresponding author: f.l.dossantos@utwente.nl

Amiet's noise prediction model [1] for foils subjected to a turbulent inflow is widely used to predict leading-edge (LE) far-field noise due to the good balance of accuracy of prediction, computational simplicity, and short computational turnaround time. This model considers an infinitely thin flat plate exposed to an inflow with turbulence. Amiet's theory also results in a formulation to determine the auto- and cross-power spectra of the wall-pressure fluctuations (WPFs) along the foil chord and span. This formulation can be used to determine the foil vibrations for vibroacoustic analysis. A significant limitation of Amiet's theory is that it does not account for the real airfoil geometric characteristics, where the foil thickness has a significant impact on the LE far-field noise. This impact is due to the inflow turbulence distortion [2]. However, limited research on the effects of turbulence distortion on the WPFs has been conducted so far [3]. Therefore, the current study aims to investigate the turbulence distortion effects on the WPFs and Amiet's WPF model.

Experiments were performed in the Aeroacoustic Wind Tunnel of the University of Twente to understand the turbulence distortion effects on the WPFs and how to account for these effects on Amiet's WPF model. The turbulent inflow was generated by a mono-planar grid, resulting in a quasi-isotropic turbulent flow with turbulence intensity of 10% and an integral length scale of approximately 50 mm at the airfoil LE position without the airfoil in the flow (undistorted values). The WPFs on a NACA 0008 and NACA 63018 (chord length $c = 300$ mm) were measured for different effective angles of attack α_{ef}. Remote microphone probes located along the chordwise and spanwise directions measured the WPFs. In addition, the turbulence characteristics of the inflow were determined from hot-wire anemometry. These measurements were conducted at the stagnation line of the airfoils for zero angle of attack at positions $-50 \leq x/r_{\mathrm{LE}} \leq -0.5$, where x is the streamwise direction with $x = 0$ at the airfoil LE and r_{LE} is the airfoil LE radius.

The experimental WPF spectrum is compared with the predictions of Amiet's WPF model at different chordwise and spanwise positions. The model formulation is presented in Eq. 18 of Paterson and Amiet [1]. The transfer function used is given by Mish and Devenport [3], and the von Kármán turbulence spectrum models the turbulent inflow. The main input to the von Kármán spectrum is the root-mean-square (RMS) of the velocity fluctuations and the longitudinal turbulence integral length scale. These parameters were determined from the hot-wire measurements for different positions upstream of the airfoil LE.

Figure 1 shows the power spectral density (PSD) of the WPFs measured (Exp.) and the spectrum predicted using Amiet's theory at two chordwise positions. G_{qq} is the one-sided PSD of the WPFs, f is the frequency, f_{ref} and p_{ref} are the reference frequency and pressure used to compute the spectrum in dB. Using Amiet's prediction, two cases are considered. The first case is the "Amiet - NTD," which refers to Amiet's model with input the turbulence parameters determined in the free stream without any influence of the airfoil. The second case "Amiet - TD" refers to Amiet's model where turbulence distortion is considered by

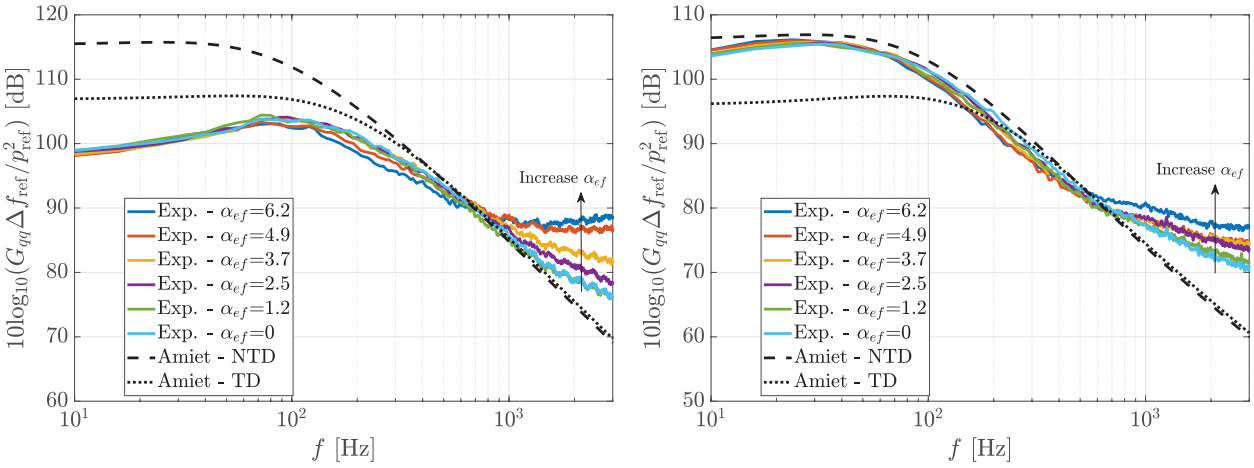

(a) $x/c = 2.12\%$ (b) $x/c = 10\%$

Figure 1: WPFs measured for different angles of attack for the NACA 0008 and predicted by Amiet's theory. $p_{\text{ref}} = 20$ µPa and $f_{\text{ref}} = 1$ Hz.

using as input the turbulence parameters determined in the vicinity of the airfoil LE at $x/r_{\text{LE}} = -2$. The turbulence parameters decrease as the airfoil LE is approached due to the turbulence distortion induced by the airfoil finite thickness.

Figure 1 shows that the angle of attack has little impact on the WPFs in the low-frequency range, but it influences the high-frequency range. For a position close to the airfoil LE ($x/c = 2.12\%$), Amiet's prediction considering the turbulence distortion (Amiet - TD) has a better agreement with the measurements for $f < 1$ kHz. However, for a more downstream position ($x/c = 10\%$), the prediction not considering the turbulence distortion (Amiet - NTD) has a better match with the measurements for $f < 600$ Hz. This behavior occurs because the turbulence distortion is mostly important in the vicinity of the airfoil LE, becoming less significant for chordwise positions that are more downstream. The disagreement for high frequencies is due to the boundary layer development and its influence on the WPFs. Similar results are observed for the NACA 63018, which will be shown in the final manuscript.

In the final manuscript, a complete description of the experimental setup and Amiet's model for the WPFs will be included. The turbulence characteristics in the vicinity of the LE of the NACA 0008 and NACA 63018 will be shown and discussed. Also, the spectral results of the WPFs for different chordwise and spanwise positions for different angles of attack for both airfoils will be analyzed. A sensitivity analysis of the turbulence input parameters for WPF predictions will be included. The results will be discussed and analyzed in detail.

References

[1] R. Paterson and R. Amiet, "Acoustic radiation and surface pressure characteristics of an airfoil due to incident turbulence," Tech. Rep. NASA CR-2733, NASA, 1976.

[2] J. Gill, X. Zhang, and P. Joseph, "Symmetric airfoil geometry effects on leading edge noise," *The Journal of the Acoustical Society of America*, vol. 134, no. 4, pp. 2669–2680, 2013.

[3] P. F. Mish and W. J. Devenport, "An experimental investigation of unsteady surface pressure on an airfoil in turbulence—part 1: Effects of mean loading," *Journal of Sound and Vibration*, vol. 296, no. 3, pp. 417–446, 2006.

Aeroacoustic source contribution to sound power for jet flows

Esmaeel Eftekharian[1], Paul Croaker[2], Richard Sandberg[3], Daniel Wilkes[4], Steffen Marburg[5], Nicole Kessissoglou[6]

[1]School of Mechanical and Manufacturing Engineering, UNSW Sydney, New South Wales 2052, Australia
Email: e.eftekharian@unsw.edu.au
[2]Platforms Division, Defence Science and Technology Group, Sydney, Australia
Email: paul.croaker1@defence.gov.au
[3]Department of Mechanical Engineering, School of Engineering, The University of Melbourne, Victoria 3010, Australia
Email: richard.sandberg@unimelb.edu.au
[4]Centre for Marine Science and Technology, Curtin University, GPO Box U1987, Perth, Western Australia 6845, Australia
Email: d.wilkes@curtin.edu.au
[5]Chair of Vibroacoustics of Vehicles and Machines, Department of Mechanical Engineering, Technische Universität München, Boltzmannstraße 15, 85748 Garching, Germany
Email: steffen.marburg@tum.de
[6]School of Mechanical and Manufacturing Engineering, UNSW Sydney, New South Wales 2052, Australia
Email: n.kessissoglou@unsw.edu.au

Jet noise is a dominant source of aircraft noise. In this work, a technique to identify the location and nature of dominant aeroacoustic sources from jet noise data is presented. The aeroacoustic source contribution technique is derived from the surface contribution technique, which was developed by Marburg et al. [1] to identify the surface areas of a vibrating structure that contribute to the far-field sound power. The surface contribution techniquewas recently extended for flow-noise problems to identify the contribution of aeroacoustic sources to the far-field sound power [2]. The aeroacoustic source contribution approach combines the Lighthill source distribution with an acoustic impedance matrix constructed from radiation kernels of the free-field Green's function, to visualize the regions of aeroacoustic sources with the greatest contribution to the far-field sound power. The method has been successfully demonstrated for simulations of co-rotating vortices and laminar flow noise around rigid cylinder [2, 3]. However, since the approach is involved with decomposition of the acoustic impedance matrix, the associated computational costs are significantly high, limiting application of the technique to simple flow structures with low grid numbers. In this work, the aeroacoustic source contribution approach is integrated with the fast multipole method (FMM) to reduce the computational cost associated with decomposition of the acoustic impedance matrix. The combined methods are implemented to determine the aeroacoustic sources in turbulent jet flow data with the greatest contribution to the far-field sound power. An overview of the aeroacoustic source contribution approach is given in what follows. The Lighthill tensor can be obtained based on flow field characteristics using:

$$\boldsymbol{T_{ij}} = \rho u_i u_j + (p - c^2\rho)\delta_{ij}, \tag{1}$$

where u_i and u_j are the i^{th} and j^{th} components of the flow velocity vector, and ρ, p are flow density and pressure, respectively. δ is the Kronecker delta and c is sound speed. Using the Lighthill tensor, $\boldsymbol{T}$, and volume of aeroacoustic sources, $\boldsymbol{V}$, the non-negative contribution of aeroacoustic sources to the far-field sound power, $\boldsymbol{\eta}$, can be obtained as follows [2]:

$$\boldsymbol{\eta_{ij}} = \frac{\mathbf{1}}{\mathbf{2}}\boldsymbol{\beta}_{\boldsymbol{ij}}^{\mathbf{T}}\boldsymbol{\beta}_{\boldsymbol{ij}}^{*}, \tag{2}$$

The superscript $^{\mathrm{T}}$ indicates the matrix transpose operator. $\boldsymbol{\beta}_{ij}$ is calculated from the eigenvalues $\boldsymbol{\Lambda}_{ij}$ and eigenvectors $\boldsymbol{\Phi}_{ij}$ of the real part of the acoustic impedance matrix $\mathrm{Re}\{\mathbf{Z}_{\mathrm{ij}}\}$, using

$$\boldsymbol{\beta}_{ij} = \boldsymbol{\Phi}_{ij}\sqrt{\boldsymbol{\Lambda}_{ij}}\boldsymbol{\Phi}_{ij}^{\mathrm{T}}\mathbf{V}\mathbf{T}_{ij}, \tag{3}$$

$$\mathbf{Z}_{ij} = \mathbf{B}_{ij}\mathbf{A}_f\mathbf{B}_{ij}^{\mathrm{H}}, \tag{4}$$

in which the superscript $^{\mathrm{H}}$ denotes the matrix Hermitian transpose. $\mathbf{B}_{ij}$ and $\mathbf{A}_f$ correspond to the double derivative of Green's function and discretized far-field surface areas, respectively. The sound power for each component of the Lighthill tensor based on the aeroacoustic source contribution method is then calculated as follows:

$$P_{ij}^{\mathrm{NNC}} = \frac{1}{2\rho c}\boldsymbol{\beta}_{ij}^{\mathrm{T}}\mathbf{V}\boldsymbol{\beta}_{ij}^{*}, \tag{5}$$

The fast multiple method has been previously adapted to the surface contribution approach for vibroacoustic applications and was shown to substantially reduce computational cost [4]. In this study, FMM in [4] is adapted to the aeroacoustic source contribution approach. To demonstrate the technique, we calculated the aeroacoustic source contributions arising from flow induced by co-rotating vortices. The results showed that dominant aeroacoustic sources are concentrated at the centre of vortex rotation in the middle of the computational domain, as shown in Figure 1.

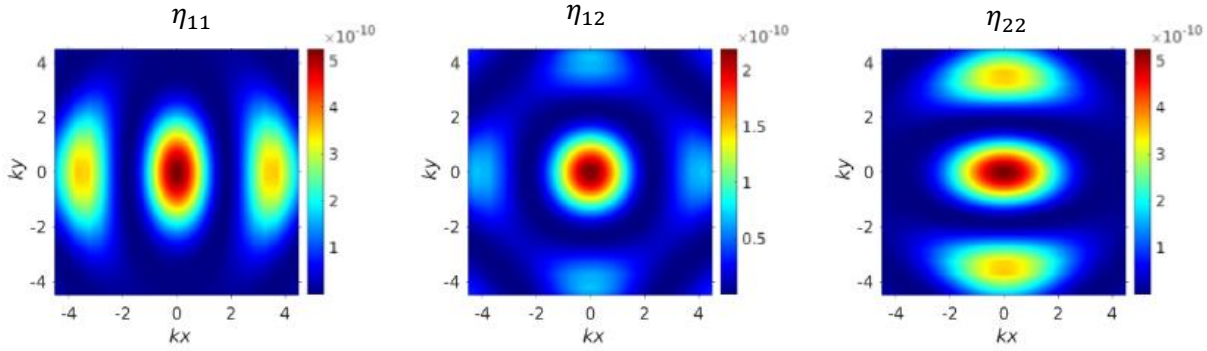

Figure 1. Non-negative contribution for different components of Lighthill tensor (Eq.2) at Mach number $= \pi/32$

Direct Numerical Simulation (DNS) velocity field of jet flow presented by Sandberg and Tester [5] is used as the flow field for acoustic analysis. This DNS data includes the velocity distribution of turbulent jet flow with a Reynolds number of 8000 (based on the nozzle diameter) discharged to a laminar co-flow. The Lighthill tensor components are calculated from this velocity distribution and combined with the integrated aeroacoustic source contribution approach to identify the location and nature of dominant aeroacoustic sources to far-field sound power.

References

[1] S. Marburg, E. Lösche, H. Peters, and N. Kessissoglou, "Surface contributions to radiated sound power," *The Journal of the Acoustical Society of America*, vol. 133, pp. 3700-3705, 2013.

[2] E. Eftekharian, P. Croaker, S. Marburg, and N. Kessissoglou, "Aeroacoustic sound contributions to sound power," in *Proceedings of Acoustics 2021*, Wollongong, Australia, 21-23 February 2022.

[3] E. Eftekharian, P. Croaker, S. Marburg, and N. Kessissoglou, "Aeroacoustic sound contribution from flow around a cylinder," in *Proceedings of the Australian Fluid Mechanics Conference*, Sydney, Australia, 4-8 December 2022.

[4] D. R. Wilkes, H. Peters, P. Croaker, S. Marburg, A. J. Duncan, N. Kessissoglou, "Non-negative intensity for coupled fluid–structure interaction problems using the fast multipole method," *The Journal of the Acoustical Society of America*, vol. 141, pp. 4278-4288, 2017.

[5] R. D. Sandberg, and B. Tester, "Mach-number scaling of individual azimuthal modes of subsonic co-flowing jets," *Journal of Fluid Mechanics*, vol. 793, pp. 209-228, 2016.

Calculating uncertainty of flow-induced vibration simulations

S.A. Hambric
Hambric Acoustics, LLC
29 March 2023

Simulating the flow-induced vibration of structures is fraught with uncertainty. Not only are structural parameters like boundary conditions and damping notoriously uncertain, but the flow induced forces are even more so. The two main approaches for estimating uncertainty are sensitivity-based and stochastic-based. Sensitivities of an output variable, such as surface-averaged vibration, with respect to uncertain inputs, such as damping or flow velocity, may be computed analytically, or numerically using finite differencing techniques. The sensitivities are combined with assumed input variable uncertainty distributions to estimate output uncertainty. The sensitivity-based method works well when the uncertainties are not cross-coupled. For flow-induced vibration, however, there are several inter-dependencies. For example, flow induced forces change with frequency, and if a structural resonance frequency is uncertain the overall uncertainty depends on the combination of structural and flow input parameters. In coupled uncertainty cases stochastic methods are simpler to apply. Uncertainty ranges and distributions, such as normal, uniform, lognormal, or others are assumed for each uncertain input. An n-dimensional random distribution of possible inputs, spanning all structural and flow input parameters, is generated and the simulation executed repeatedly for each set of inputs. The output response distributions are then available to plot and examine, along with global sensitivities – which show which input variables have the most impact on the output variability. In this paper I demonstrate these uncertainty principles on the vibration of Blake and Maga's cantilevered strut excited by turbulence ingestion flow in a water tunnel [1]. I examine uncertainty in structural parameters which affect resonance frequency and hydrodynamic damping (a cross-coupled uncertainty!) and flow parameters like mean velocity, turbulence intensity, and integral length scale. The simulated vibrations at resonance, spanned by the resulting uncertainties (computed using a Microsoft Excel plugin called Argo from Booz Allen Hamilton [2]) agree well with measurements.

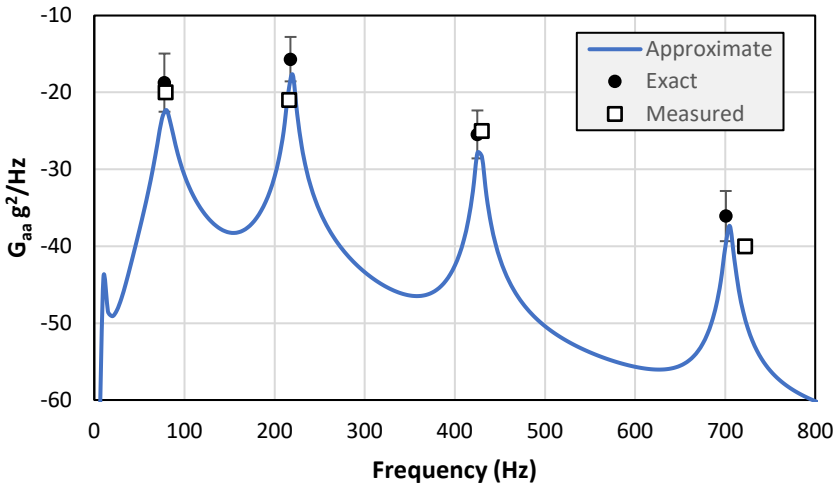

Figure 1. Measured and simulated strut vibration at U=7.2 m/s, including 95% confidence intervals.

1. Blake, W., and Maga, L., *Vibratory Dynamics of Flow-Excited Struts in Water*, NSRDC Report 4087, 1973.
2. ARGO, Booz Allen Hamilton, https://boozallen.github.io/argo/

Acoustic metaliner for sound insulation in a duct with flow

Wonju JEON[1]

[1]Department of Mechanical Engineering, Korea Advanced Institute of Science and Technology, Republic of Korea
Email: wonju.jeon@kaist.ac.kr

Abstract

We present a metaliner design with the goal of reducing noise in ducts while minimizing flow resistance. The unit cell of metaliner is composed of two different sub-wavelength Helmholtz resonators (HRs) to derive hybrid, which results in high absorption upstream direction as well as high transmission loss in downstream direction. For fast and accurate design of the metaliner, a theoretical model is established to determine the effective acoustic impedance of the metaliner with the influence of flow, predicting the sound insulation performance in a duct with grazing flow. The metaliner is designed to provide high transmission loss at a target frequency for different flow speeds. The experimental results show that the designed metaliner exhibits a high transmission loss per unit length of over 45 dB/m with a wide bandwidth (10% of the target frequency) for different flow speeds of 0, 17, and 34 m/s.

1. Introduction

Noise attenuation in ducts is important for various industrial applications, including the ventilation system of vehicles and the air intake system of cooling towers. Nevertheless, conventional acoustic treatments, such as acoustic mufflers or louvers, have been commonly utilized to reduce duct noise (1), they not only provide poor attenuation at low-frequency but also obstruct airflow passages, causing the degradation of product functionality. To overcome those limitations, the developments of acoustic metamaterials that offer low-frequency sound insulation without the obstruction of fluid passage have been carried out (2). However, previous studies have focused only on achieving high sound insulation performance in stationary media, failing to ensure sound insulation in ducts with flow. Therefore, this study proposes a metaliner design aimed at insulating duct noise in the presence of grazing flow. A theoretical model that considers the effect of flow on the effective impedance of the metaliner is established based on a recent study (3-4). Using the theoretical model and numerical simulation, the transmission loss of the metaliner in a duct is predicted for different flow speeds. The metaliner is then designed to demonstrate high transmission loss per unit length of more than 45 dB/m with a bandwidth of 10% of the target frequency for flow speeds of 0, 17, and 34 m/s. Finally, the metaliner is fabricated via 3D printing, and its sound insulation performance is validated experimentally.

2. Result and discussion

Figure 1(a) illustrates a schematic representation of a metaliner that reduces noise in ducts with little flow resistance. Figure 1(b) shows the geometry of the metaliner, which is composed of two different

sub- λ HRs arranged alternately on the bottom of the rectangular duct with dimensions of 406 mm × 51 mm × 30 mm.

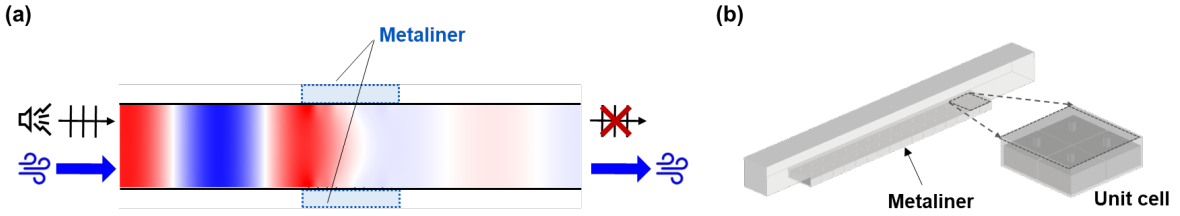

Figure 1: (a) Schematic representation of metaliners. (b) Geometry of a metaliner installed under a rectangular duct.

Figure 2 shows the transmission loss and absorption coefficient spectra of the designed metaliner for different average flow speeds ($\bar{U}$ = 0, 17, and 34 m/s) at a target frequency of 500 Hz. As shown in Fig. 2. the results obtained from the experiment and simulation are in good agreement. The experimental results show that the metaliner can yield high transmission loss per unit length of more than 45 dB/m with a bandwidth of 10% of the target frequency for different flow speeds. Also, high sound insulation was realized even at other flow speeds ranging between 0 and 34 m/s, as detailed in reference (5).

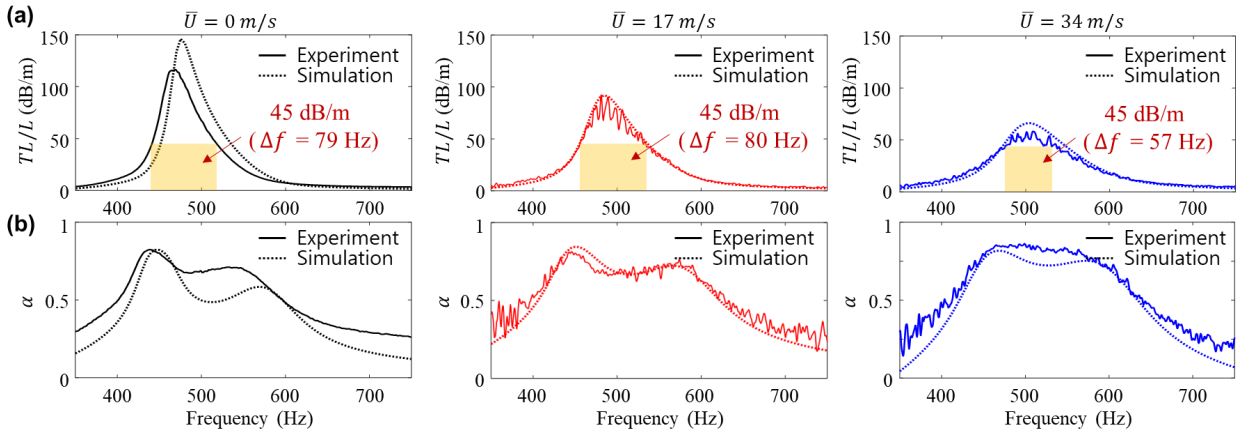

Figure 2: (a) Transmission loss per unit length and (b) absorption coefficient of the designed metaliner (target frequency: 500 Hz) for different flow speeds of 0, 17, and 34 m/s.

References

[1] E. B. Viveiros, B. M. Gibbs, S. N. Y. Gerges, Measurement of sound insulation of acoustic louvers by an impulse method, Appl. Acoust., 63 (2002) 1301-1313.

[2] R. Ghaffarivardavagh, J. Nikolajczyk, S. Anderson, and X. Zhang, Ultra-open acoustic metamaterial silencer based on Fano-like interference, Phys. Rev. B, 99 (2019) 024302.

[3] H. Ryoo and W. Jeon, Dual-frequency sound-absorbing metasurface based on visco-thermal effects with frequency dependence, J. Appl. Phys., 123 (2018) 115110.

[4] H. Ryoo and W. Jeon, Perfect sound absorption using ultra-thin metasurface based on hybrid resonance and space-coiling, Appl. Phys. Lett., 113 (2018) 121903.

[5] T. S. Oh and W. Jeon, Acoustic metaliners for sound insulation in a duct with little flow resistance, Appl. Phys. Lett., 120 (2022) 044103.

Measurements of wavenumber-frequency spectra in an open-jet pressure gradient facility

Chaoyang Jiang[1*], Con Doolan[1], Charitha de Silva[1] and Danielle Moreau[1]

[1]Flow Noise Group, School of Mechanical and Manufacturing Engineering
UNSW, Sydney 2052, Australia
[*]Email: chaoyang.jiang@unsw.edu.au

Pressure gradients are often present in real-world turbulent flows, such as turbulent boundary layers that develop over curved surfaces and wall-bounded turbulent flows with varying cross-sectional area. The knowledge of surface pressure fluctuations associated to these flows is essential for accurate predictions of flow-induced noise (e.g., trailing-edge noise) in practical applications. This paper characterises the surface pressure fluctuations beneath the turbulent boundary layers on a newly developed open-jet facility, which can generate controllable pressure gradients. Point auto-spectra and wavenumber-frequency spectra of the unsteady surface pressure are obtained using a remote microphone technique and compared with published results from other facilities [1].

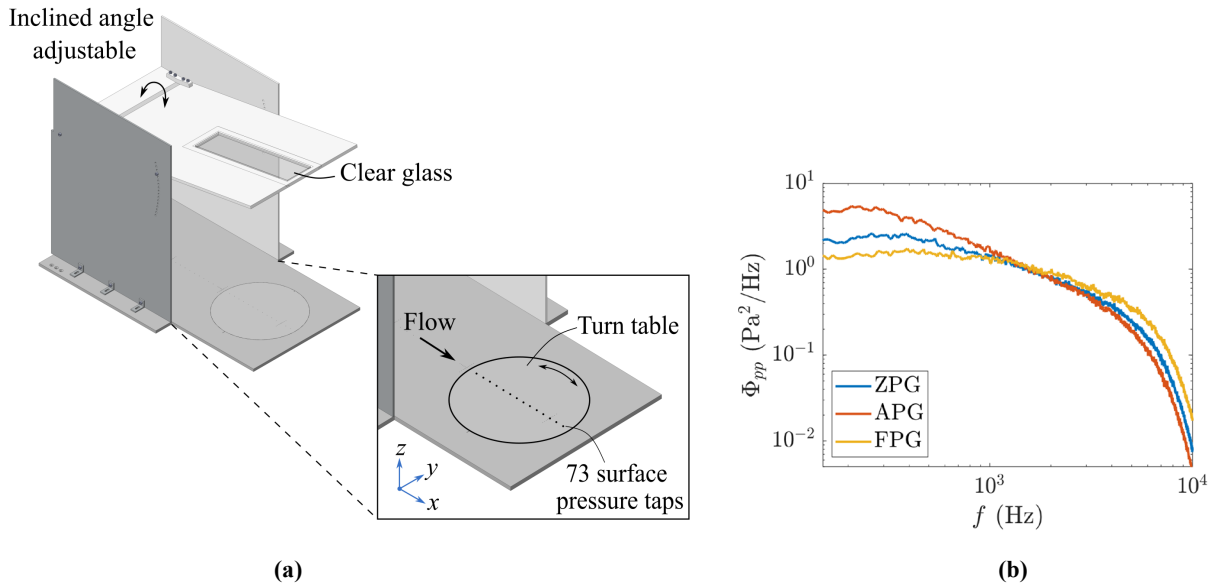

(a) **(b)**

Figure 1: (a) Schematic of the experimental setup of the fluctuating surface pressure measurements at the open-jet pressure gradient test rig. (b) Surface pressure spectra beneath turbulent boundary layers with ZPG, APG and FPG.

Measurements are performed on an open-jet pressure-gradient test rig at the UNSW Anechoic Wind Tunnel. Various pressure gradients are created by adjusting the inclination angle of the top-plate to gradually increase/decrease the cross-sectional area of the open jet test section along the streamwise direction (see Figure 1a). Two side plates are installed to help maintain the pressure gradient, and a circular turn table is installed immediately downstream of the slide plates. A line array of 73 surface pressure taps is implemented to the turn table for surface pressure measurements. Experiments are performed at a freestream velocity U_∞ = 30 m/s and top-plate inclination angles α_t = −8°, 0° and 8°, corresponding to favourable-, zero-, and adverse-pressure gradients, namely FPG, ZPG and APG. The boundary layer

profiles and static pressure distributions along the bottom-plate centre line are characterised using PIV and surface pressure taps. The Clauser pressure gradient parameter β of FPG, ZPG and APG flows are −0.19, 0 and 0.60, respectively, and the pressure gradients for APG and FPG flows are both approximately linear. Figure 1b presents the auto-spectra of the surface pressure fluctuations measured at the center of the turn table under flows with different pressure gradients. APG induces more intense pressure fluctuations at low frequencies due to the large-scale motions associated with it, while FPG increases the intensity of high-frequency pressure fluctuations. The wavenumber-frequency spectra are obtained through angular sweep measurements of the surface pressure fluctuations at the line array of taps on the turn table. The sweep ranges from 0° to 175° in 5° increments with a total of 73×36 = 2628 measurement points. The calculation of wavenumber-frequency spectrum follows the procedure proposed in [2], and the results will be presented in the full paper.

References

[1] É. Salze, C. Bailly, O. Marsden, E. Jondeau and D. Juvé, “An experimental characterisation of wall pressure wavevector-frequency spectra in the presence of pressure gradients," in *20th AIAA/CEAS Aeroacoustics Conference* (p. 2909), 2014.

[2] B. Arguillat, D. Ricot, C. Bailly and G. Robert, “Measured wavenumber: Frequency spectrum associated with acoustic and aerodynamic wall pressure fluctuations, " *The Journal of the Acoustical Society of America*, 128(4), 1647-1655, 2010.

Acoustic source localisation from vibration measurement of a plate beneath a turbulent boundary layer

Mahmoud Karimi[1] and Laurent Maxit[2]

[1]Centre for Audio, Acoustics and Vibration,
University of Technology Sydney, Sydney, Australia
e-mail: Mahmoud.karimi@uts.edu.au
[2]Univ Lyon, INSA Lyon, LVA, 25 bis, av.
Jean Capelle, 69621, Villeurbanne Cedex, France
e-mail: Laurent.maxit@insa-lyon.fr

Microphone arrays have been widely used for acoustic source localisation in many different applications. This has been done by measuring sound pressure and applying the acoustic beamforming to the pressure signals to localise the source. In some cases, when the microphone array is placed on a surface and is exposed to a turbulent flow (see Fig. 1(a)), the ability of the array to localise the acoustic source (signal) can be significantly diminished as the signal will be masked by the background noise induced by the turbulent flow. Hence, this work introduces an alternative technique for acoustic source localisation in the presence of a turbulent boundary layer (TBL). The technique is based on a vibroacoustic beamforming which applies the beamforming procedure to the measured vibration signals at the surface of a structure in contact with the fluid in which the acoustic source is located (see Fig. 1(b)).

This work will study the ability of the vibroacoustic beamforming to improve the source localisation in comparison with acoustic beamforming. This will be achieved by exploiting spatial filtering of the structure which filters the most energetic components (convective ridge) of the TBL excitation at frequencies well above the aerodynamic coincidence frequency (i.e. at the frequency when the flexural wavenumber equals the convective wavenumber). In order to evaluate the performance of the proposed vibroacoustic beamforming, a numerical model of an elastic plate under TBL/monopole excitation is considered and the results of vibroacoustic beamforming are compared against the corresponding results obtained by acoustic beamforming using microphone array located on a rigid plate. The effectiveness of each method is then assessed by quantifying the dynamic range and spatial resolution for each technique.

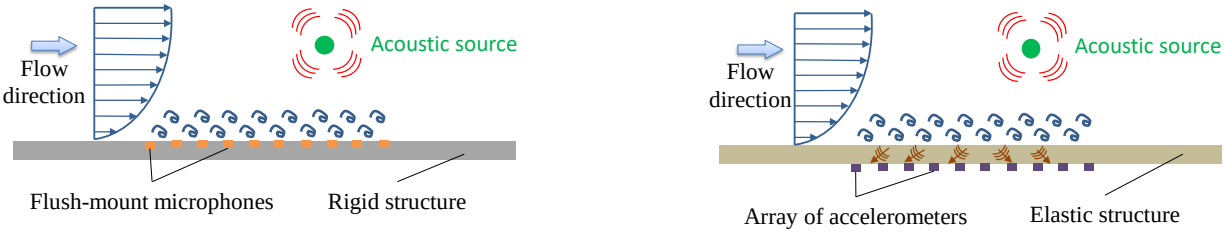

Figure 1. Schematic diagram for source localization in the presence of a turbulent boundary layer using (a) microphone array (acoustic beamforming) and (b) accelerometer array (vibroacoustic beamforming).

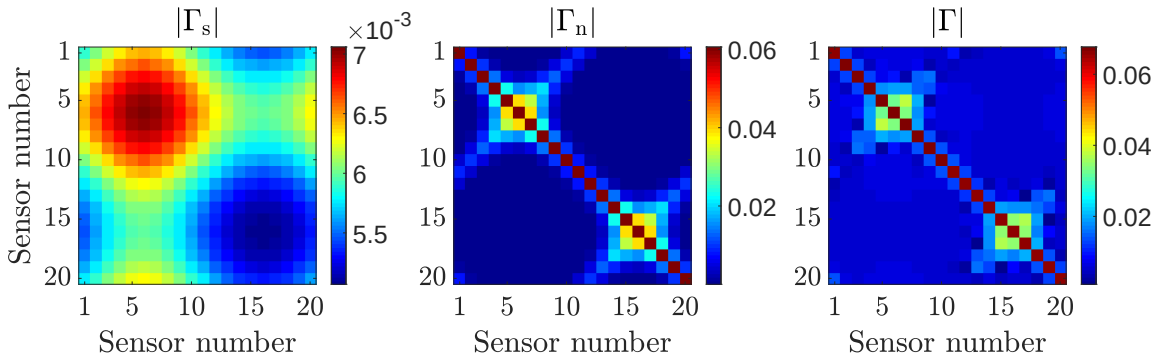

(a) CSM of the signals measured by the microphones

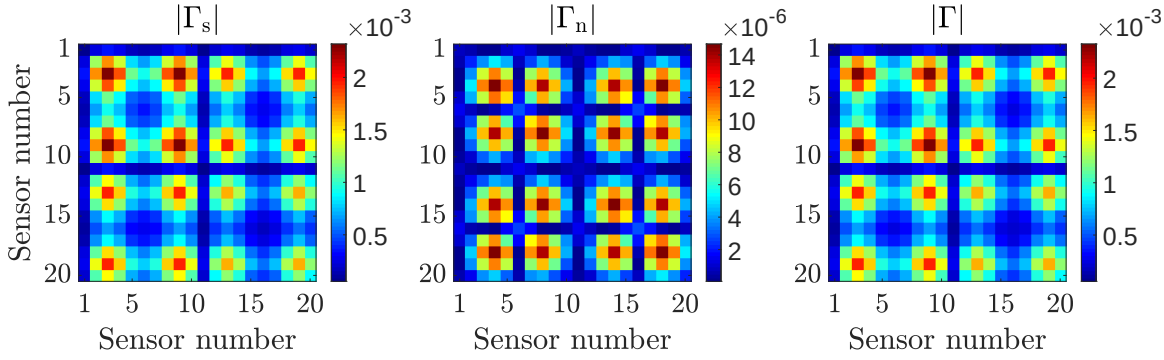

(b) CSM of the signals measured by the accelerometers

Figure 2. Maps of the CSM using circular array of 20 sensors at 700 Hz. The CSMs of (a) the acoustic pressures using microphone array (b) the vibratory field using accelerometer array induced by the acoustic source ($|\Gamma_s|$), noise ($|\Gamma_n|$) and both source and noise ($|\Gamma|$).

One of the key parameters in the beamforming is signal-to-noise ratio (SNR) which directly affects beamforming performance in source localisation. It should be noted that for the acoustic beamforming the SNR is defined as the ratio expressed in dB of the auto spectrum density (ASD) of the blocked pressure induced by the source to be localised, over the ASD of the TBL wall pressure field. However, in the vibroacoustic beamforming, the SNR is defined as the ratio expressed in dB of the ASD of the acceleration induced by the source to be localised, over the ASD of the acceleration induced by the TBL wall pressure field. To show why the vibroacoustic beamforming could have better localisation performance than acoustic beamforming in the presence of a TBL, let us consider the source localisation problem illustrated in Fig. 1 with a circular array of 20 sensors (microphones/accelerometers) and flow speed of 60 m/s. Fig. 2 shows cross spectrum matrix (CSM) of the signal ($|\Gamma_s|$), noise ($|\Gamma_n|$) and signal plus noise ($|\Gamma|$) for all the sensors at 700 Hz. It can be seen that the background noise is much higher than the signal from the source (see Fig. 2(a)) when using the microphone array. On the contrary, since the structure filters the convective ridge of the TBL excitation, using vibration approach the acceleration induced by the TBL (noise) is lower than that induced by the acoustic source (signal) (see Fig. 2(b)). Therefore, for the same configuration, vibroacoustic beamforming will have a higher SNR than acoustic beamforming and this could result in a better performance in source localisation. This aspect will be investigated in details and the results will be presented at Flinovia 2023.

Porous edges for flow noise reduction: from theory to application

John R. Kershner[1], Justin W. Jaworski[2], and Thomas F. Geyer[3]

[1,2]Department of Mechanical Engineering and Mechanics, Lehigh University
19 Memorial Drive West, Bethlehem, PA 18015, United States of America
e-mail: jrk520@lehigh.edu, jaworski@lehigh.edu
[3]Brandenburg University of Technology Cottbus-Senftenberg, 03046 Cottbus, Germany
e-mail: thomas.geyer@b-tu.de

The recent reexamination of quiet owl flight by the aeroacoustics community has led several researchers to explore how material or geometric aspects of avian wings could enable passive aerodynamic noise reduction in low-speed flows [1]. However, a leading barrier to understanding and translating avian wing features to engineering application is the broad design space engendered by the complex construction of avian wings and the myriad ways in which their physical details may be characterized or realized in either a model or an experiment. Among the several approaches to idealize avian wing features, their representation as a homogenized porosity condition enables their description in terms of only a few physical parameters and facilitates the construction and solution of theoretical models to direct computational or experimental validation of the noise generation processes.

Predictive analyses for noise scattered by porous surface [2] or edges [3] suggest that the radiated acoustic field depends on a single dimensionless parameter only. Small values of this porosity parameter recover the well-known fifth-power acoustical power scaling on flight speed and the cardioid directivity of the acoustic pressure field, which at large parameter values shift simultaneously to a sixth-power flight speed scaling and a dipolar directivity, respectively. The weaker sound produced by porous edges complicates experimental validation of these results when using a standard aeroacoustic tunnel, whose background noise scales similarly to a highly-porous edge. To circumvent this issue, recent theoretical analysis [4] using a vortex ring source in a quiescent fluid in lieu of a mean flow provides an alternative strategy for experimental confirmation of directivity and acoustic power scaling results for porous edges, as well as producing additional metrics and time-dependent acoustic predictions to validate a vortex-ring noise measurement. Ongoing efforts to connect theoretical and experimental campaigns are expected to support the development of a predictive and scientific understanding of porosity on edge noise, with a view to translate this knowledge to engineering application in low-speed flows.

The present work focuses on current developments to bridge basic science investigations for the acoustics of porous edges to physical demonstrations and eventual engineering application, whose progession is illustrated schematically in Figure 1. Supposing confirmation of the single dimensionless porosity parameter as an appropriate way to describe porous edge noise, a natural follow-on concern is how one sets about designing and implementing the porosity on a wing in a practical sense. This task also brings into question the robustness of the single-parameter description to real flow effects, which have been disregarded in the theoretical modeling and avoided in controlled experiments. Furthermore, porous surfaces and edges designed for passive flow noise control may be affected by the local mean flow and could affect the aerodynamics in a modest but noticeable way when translated to a lifting surface. i.e., a wing or wind turbine blade, among other candidate applications. An overview of physics-informed investigations of porosity designs for edge noise will be made in the full article, including recent attempts to measure noise on a flight vehicle at the owl scale, extensions of existing works to investigate non-uniform porosity distributions on the aerodynamics and acoustics, and the identification of opportunities to explore the fluid mechanics of porous edge designs.

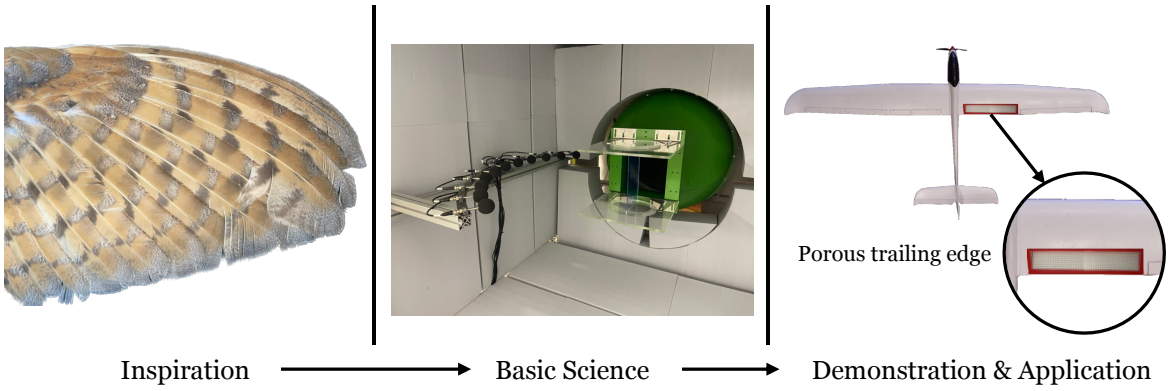

Figure 1: A biologically-informed engineer's approach to reduce noise using porosity. The porous planform of the owl wing (left) and the analyses it inspired leads to focused wind tunnel tests with porous plates for validation of the physical mechanisms (middle), which are then adapted for small-scale aircraft with porous trailing edges to assess real flow and aerodynamic effects (right).

References

[1] J. W. Jaworski and N. Peake, "Aeroacoustics of silent owl flight," *Annual Review of Fluid Mechanics*, vol. 52, pp. 395–420, 2020.

[2] J. E. Ffowcs Williams, "The acoustics of turbulence near sound-absorbent liners," *Journal of Fluid Mechanics*, vol. 51, no. 4, pp. 737–749, 1972.

[3] J. W. Jaworski and N. Peake, "Aerodynamic noise from a poroelastic edge with implications for the silent flight of owls," *Journal of Fluid Mechanics*, vol. 723, pp. 456–479, 2013.

[4] H. Chen, Z. W. Yoas, J. W. Jaworski, and M. H. Krane, "Acoustic emission of a vortex ring near a porous edge. Part 1: theory," *Journal of Fluid Mechanics*, vol. 941, A28, 2022.

Aeroacoustic noise produced by small unmanned aerial vehicle propellers

Michael J. Kingan[1], Sung Tyaek Go[1], Yan Wu, Riul Jung, and Ryan S. McKay[1,2]

[1]Acoustics Research Centre, Department of Mechanical Engineering, The University of Auckland
20 Symonds Street, Auckland 1010, New Zealand
Email: m.kingan@auckland.ac.nz, sgo587@aucklanduni.ac.nz

[2]Dotterel Technologies Ltd.
16/930 Great South Road, Auckland 1061, New Zealand
Email: ryan.mckay@dotterel.com

Multi-rotor unmanned aerial vehicles (UAVs) are becoming increasingly common. Small (<5 kg) commercially available UAVs typically have four or six rotors, each of which have two blades and a diameter of less than 0.4 m. The noise produced by these vehicles is due primarily to the aeroacoustic loading sources on the surface of the blades of the rotors [1]. The steady component of the loading produces tones at harmonics of the blade passing frequency of the propellers. The unsteady loading can be caused by a number of different physical mechanisms, including unsteady blade motion, a turbulent inflow, and the interaction of the blades with a flow distortion (produced, for example, by an adjacent strut).

We believe that the unsteady loading produced by a turbulent inflow onto the propeller is an important source of noise for these propellers when operating in hover. A rotor operating in hover will produce a very strong stream-tube contraction which draws in turbulent eddies from a wide volume above the rotor which are elongated as they pass through the contraction. A schematic showing this process is shown in figure 1 (left). These elongated turbulent eddies can be 'chopped' many times by the rotor blades as they pass through the rotor producing correlated unsteady loading on the air with each chop. This correlated loading will produce a sound pressure level spectrum which contains a multitude of narrow peaks. We have conducted experimental measurements of the sound pressure level spectrum of a single 0.38 m diameter UAV propeller operating in isolation in the large anechoic chamber at the University of Auckland. The sound pressure level spectrum measured at a location directly above the propeller is shown in figure 1 (right) and is observed to contain a multitude of peaks consistent with turbulent inflow noise. This spectrum is also qualitatively similar to one measured outdoors which is also shown in this figure.

This presentation will describe analytical models which have been developed for predicting this noise source. These models utilise rapid distortion theory to model the elongation of the turbulent eddies as they pass through the stream tube contraction; thin aerofoil theory to model the unsteady loading response of the propeller blades; and an analytical model for calculating the sound radiation. The full model is

computationally expensive to evaluate, and techniques for reducing the computational time will be presented. Comparison of the predictions with experimental measurements will also be presented.

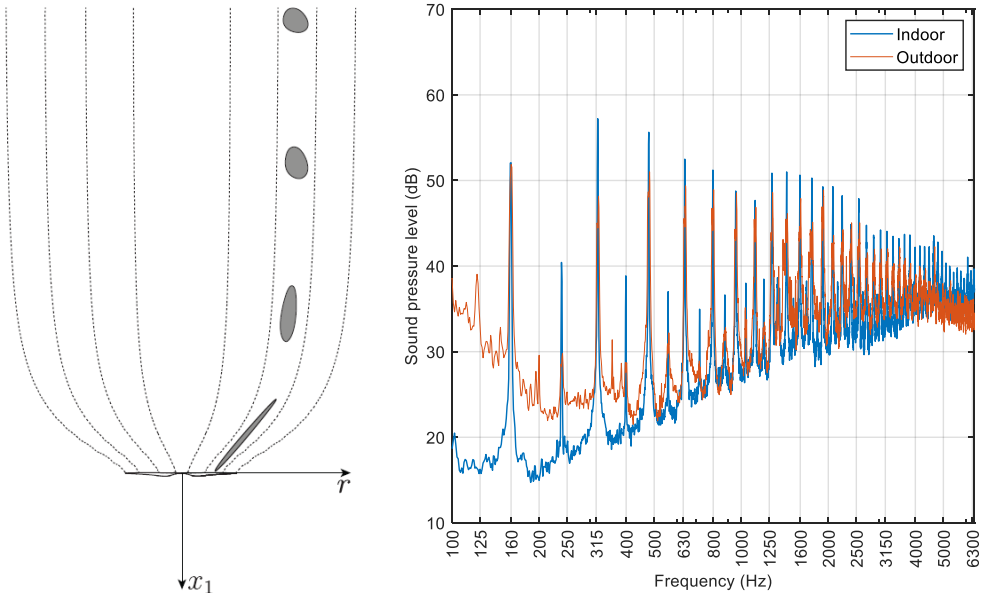

Figure 1: Schematic showing turbulent eddies being elongated in the inflow to the rotor (left). Narrow-band sound pressure level spectra produced by a UAV rotor operating inside an anechoic chamber and outdoors (right).

An analytical model has also been developed to predict the turbulent inflow noise produced by a shrouded propeller [2] and predictions made using this model will be presented which are compared with measurements conducted in the low noise wind tunnel at the University of Bristol.

This presentation will also describe work undertaken to assess the tonal noise produced by a UAV propeller with an adjacent strut [3], the tonal noise produced by a shrouded propeller, the noise produced by a contra-rotating UAV propeller [4] and recent work to design a quiet contra-rotating propeller.

References

[1] C. T. J., M. J. Kingan, Y. Hioka, G. Schmid, G. Dodd, K. N. Dirks, S. Edlin, S. Mascarenhas, Y.-M. Shim, “Quantification of the psychoacoustic effect of noise from small unmanned aerial vehicles," *International Journal of Environmental Research and Public Health*, vol. 18, paper no. 8893, 2021.

[2] S. T. Go, M. J. Kingan, R. S. McKay, R. N. Sharma (2023) Turbulent inflow noise produced by a shrouded propeller, Journal of Sound and Vibration, vol. 542, paper no. 117366

[3] Y. Wu, MJ Kingan, ST Go, Propeller-strut interaction tone noise, Physics of fluids, 34(5), 055116

[4] R. Jung, M. J. Kingan, P. Dhopade, R. N. Sharma, R. S. McKay, Investigation of the Interaction Tones Produced by Contra-Rotating Unmanned Aerial Vehicle Rotor Systems, AIAA Journal, pp. 1-16, 2023

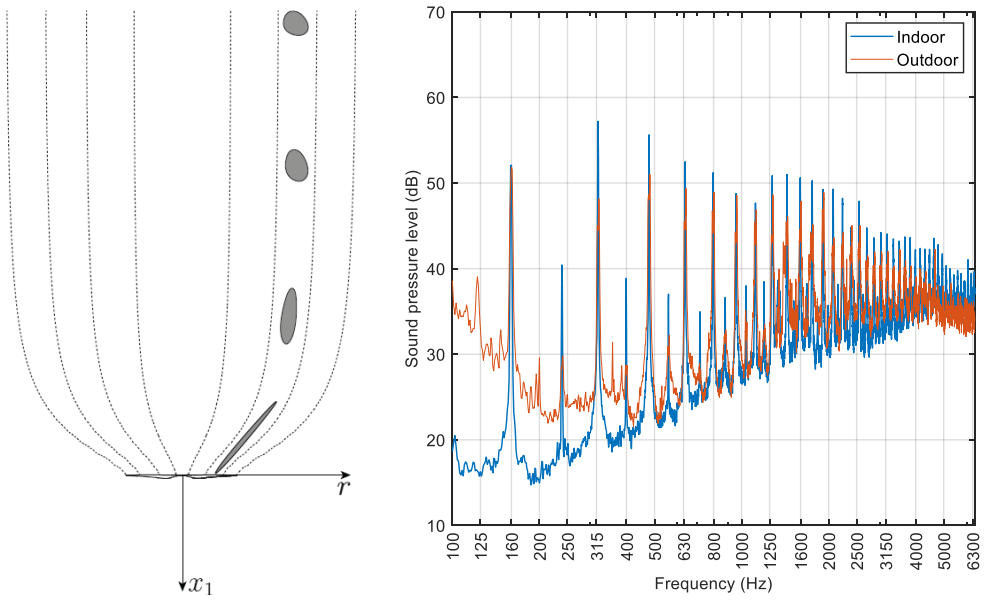

Figure 1: Schematic showing turbulent eddies being elongated in the inflow to the rotor (left). Narrow-band sound pressure level spectra produced by a UAV rotor operating inside an anechoic chamber and outdoors (right).

References

[1] C. T. J., M. J. Kingan, Y. Hioka, G. Schmid, G. Dodd, K. N. Dirks, S. Edlin, S. Mascarenhas, Y.-M. Shim, “Quantification of the psychoacoustic effect of noise from small unmanned aerial vehicles," *International Journal of Environmental Research and Public Health*, vol. 18, paper no. 8893, 2021.

Noise Emissions from Cavitation Inception During the Interaction of a Pair of Line Vortices

Daniel Knister[1], Harish Ganesh[2], Steven L. Ceccio[1,2]
[1]Department of Mechanical Engineering, University of Michigan-Ann Arbor
1231 Beal Ave, Ann Arbor MI, 48109, United States of America
Email: dknister@umich.edu
[2]Department of Naval Architecture and Marine Engineering, University of Michigan-Ann Arbor
2600 Draper Dr, Ann Arbor, MI 48109, United States of America
Email: gharish@umich.edu

Introduction

Cavitation is typically undesirable in hydrodynamic flows, and designers often work to mitigate or prevent its occurrence. Generally, the regions that cavitate first on a vessel are its lifting surfaces, where there are typically free shear flows containing an array of vortical structures of various sizes and orientations. The core of a single vortex has a reduced pressure (and even tension in liquids) relative to its surroundings. When multiple vortices interact, there can be an additional reduction in core pressure, leading to inception. The weaker (e.g. lower circulation), "secondary" vortices often cavitate first in real world flows (Katz and O'Hern 1986). This is because the weaker vortices are stretched by the stronger vortices, leading to a transient drop in the core pressure of the weaker vortices. As a canonical example of this phenomenon, a pair of unequal strength, initially parallel, counter-rotating line vortices is considered. Because of the long wavelength Crow instability (Crow 1970), the weaker of the two vortices is stretched substantially, leading it to cavitate before the stronger vortex.

This experimental study uses Shake-the-Box (STB) (Schanz et al. 2016), a volumetric Lagrangian Particle Tracking Velocimetry (PTV) technique to measure the two vortices. These measurements are used to estimate the instantaneous vortex stretching and the pressure drop in the cores of the vortices, measurements unavailable in the previous study by Chang et al. (2012). The distribution of transient drops in pressure are found and related to the stretching of the vortex and compared to the steady component of the reduction in pressure due to the presence of a vortex. In conjunction with these measurements, a Cavitation Susceptibility Meter is used to characterize the nuclei distribution in the water. Between the estimated vortex core pressure drop from the PTV measurements and the nuclei distribution from the CSM, the rate of inception events is estimated and compared to the experimentally observed inception rate. The acoustic emissions of incepting bubbles are related to the vortical flow as well.

Experimental Approach

The experiments are conducted in the University of Michigan's Miniature Large Cavitation Channel, a recirculating water channel with variable speed and pressure. All experiments are conducted at 10 m/s. A pair of cambered hydrofoils is used to generate the vortices creating the interaction and cavitation. The foils' angles of attack and spacing can be changed to change the vortex properties and the resulting interaction.

The interaction of the vortices is measured using PTV in two regions at approximately 0.7 and 1.5 chords downstream of the foils, where inception is most likely to occur. A Photonics Dual Head DM100-532 laser is used to illuminate the volume while images are recorded with 4 Phantom v1212 cameras. The cameras are arranged on both sides of the tunnel due to space constraints.

Results and Discussion

Initial measurements of the cavitating vortex flow were taken with high-speed video in combination with a hydrophone. Figure 1 shows an image of the two interacting vortices visualized by developed cavitation. The weaker vortex is seen undergoing its instability, turning and being stretched. At higher pressure, the developed cavitation is suppressed, but incipient cavitation can occur. Volumetric velocimetry measurements of the vortex interaction process were obtained at 15 kHz. The STB data was processed with LaVision's DaVis software, using their proprietary VIC# to calculate Eulerian pressure and velocity fields from the Lagrangian particle data. It is found that strain along the vortex axis is correlated with a reduction in pressure (will be discussed in the presentation). Figure 2 shows inception occurring in the weak secondary vortex and its associated acoustic emission. Explosive growth of the nucleus results in the acoustic pressure signatures recorded by the hydrophone. Observed inception cavitation number and the acoustic signature depend on the background nuclei content. In the presentation, we will present the relationship between the underlying properties of the stretched vortex, background nuclei distribution, observed inception rate, and the acoustic signature.

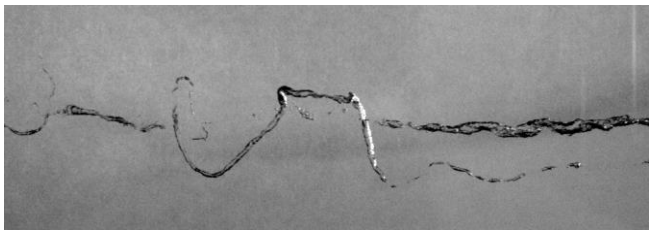

Figure 1: Image of the two interacting vortices visualized by developed cavitation.

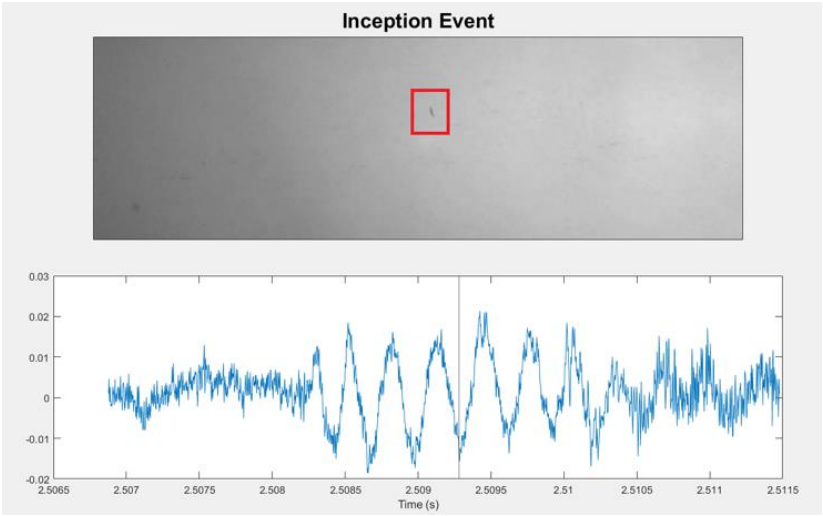

Figure 2: An inception bubble in the stretched secondary is shown above its acoustic emission. The incepting bubble is outlined in red and the moment the image was taken is identified by the vertical line on the hydrophone trace

Conclusion

The instability studied here is the simplest possible case of the vortex stretching induced cavitation inception that characterizes turbulent shear flows in real naval vessels. Using STB PTV, the pressure and stretching in the cores of stretched vortices are quantified and related to the acoustic emissions. Stretching is clearly shown to drive the reduction in pressure in the core of the weaker vortices. This information about the pressure history in the vortex cores, in combination with the nuclei distribution found from the CSM allows prediction of the inception event rate.

Efficient Large-Eddy Simulation Methods for Predicting Wall-Pressure Fluctuations Beneath a Turbulent Boundary Layer

Graeme Lane[1,2*], Paul Croaker[2], and Marcus Winroth[3]

[1]Mechanical and Automotive Engineering, RMIT University, GPO Box 2476, Melbourne, Victoria, 3001, Australia
[2]DST Group, 506 Lorimer Street, Fishermans Bend, Victoria, 3207, Australia
[3] FOI, Totalförsvarets forskningsinstitut, 164 90 Stockholm, Sweden
*Email: graeme.lane@rmit.edu.au

Prediction of flow-induced noise is important for a wide range of engineering applications. An important source of flow noise comes from the pressure fluctuations beneath a turbulent boundary layer as they interact with the surface or scatter from sharp edges to produce far-field sound. Prediction of this noise, using acoustic analogy methods such as the Ffowcs-Williams & Hawking or Amiet models, requires knowledge of these pressure fluctuations.

Computational fluid dynamics (CFD) methods may provide a means to predict the pressure fluctuations. However, the commonly used approach based on the Reynolds-averaged Navier-Stokes (RANS) equations does not provide any direct information about pressure fluctuations. Instead, a scale-resolving method is required. Large eddy simulation (LES) methods are often employed to reduce the very large computational cost of such simulations, by resolving only larger turbulent structures while modelling smaller scales. However, when applied to a boundary layer, LES is still very expensive, due to the need to resolve large eddy structures of diminishing length scale approaching a wall. Instead of wall-resolved LES (WRLES), the cost may be reduced by adopting wall-modelled LES (WMLES), which permits resolving only eddies in the outer region of the boundary layer, which scale with the boundary layer thickness.

The accuracy of wall-modelled LES (WMLES) methods for predicting pressure fluctuations has been compared with wall-resolved LES (WRLES), using turbulent channel flow as a test case. Simulations were carried out using the open-source software OpenFOAM. Computational meshes for the channel flow simulations were constructed in accordance with recommendations from the literature to ensure that cell sizes were small enough to resolve the large eddy structures. For WRLES, this meant that the mesh spacing must be very fine approaching the walls. On the other hand, the mesh for WMLES can be uniformly spaced in the wall-normal direction. As a result, the mesh for WRLES had a total of 25 million cells at friction Reynolds number, $Re_\tau = 1000$, and 95 million cells at $Re_\tau = 2000$. For WMLES, the mesh was about 3 million cells regardless of Reynolds number. To compensate for the absence of the near-wall small eddy structures in WMLES, a “wall function” (WF) was introduced, to provide the correct shear stress at the wall.

Two approaches were investigated for WMLES. In the first approach, the LES equations were solved throughout the computational domain, applying the WALE eddy viscosity model to account for sub-grid turbulence scales (this method is referred to as WMLES-WF/WALE). The second approach adopts a hybrid RANS-LES turbulence model, where LES is applied only in regions away from walls where the mesh spacing is adequate for resolving large eddy structures, while the RANS equations are solved in regions adjacent to the wall. For this purpose, the Improved Delayed Detached Eddy Simulation (IDDES) model [1] was adopted (this method is referred to WMLES-WF/IDDES).

The accuracy of WRLES and the first WMLES method (WMLES-WF/WALE) applied to channel flow has been previously evaluated by Liefvendahl et al. [2]. Reasonable predictions of mean and fluctuating velocity profiles were obtained. WRLES also gave quite accurate predictions for the power spectral

density (PSD) of the pressure fluctuations, but the WMLES method resulted in substantial overprediction (as illustrated in Figure 1). The revised WMLES approach (WMLES-WF/IDDES) significantly improves the prediction of near-wall pressure fluctuations. Figure 1 shows that the wall-pressure PSDs with this method showed good prediction of low-to-medium frequencies associated with the resolved turbulence in the outer region of the boundary layer. A premature decay is observed at higher frequencies, as these frequencies are mainly generated in the inner part of the boundary layer where turbulence is suppressed by activation of the RANS equations. Nevertheless, the WMLES-WF/IDDES approach shows substantial improvement over the WMLES-WF/WALE method, while also providing substantial computational savings compared to WRLES.

Further development is in progress. Firstly, the revised WMLES method is being applied to more realistic engineering applications, such as the flow over a NACA0012 aerofoil. As well as predicting the surface pressure fluctuations, the wall-pressure PSD will be used to predict the trailing-edge noise. An additional consideration is the prediction of the missing higher frequencies in the wall-pressure PSD. It may be possible to extend the spectrum using a semi-analytical model based on a solution to the pressure Poisson equation (see Grasso et al. [3]).

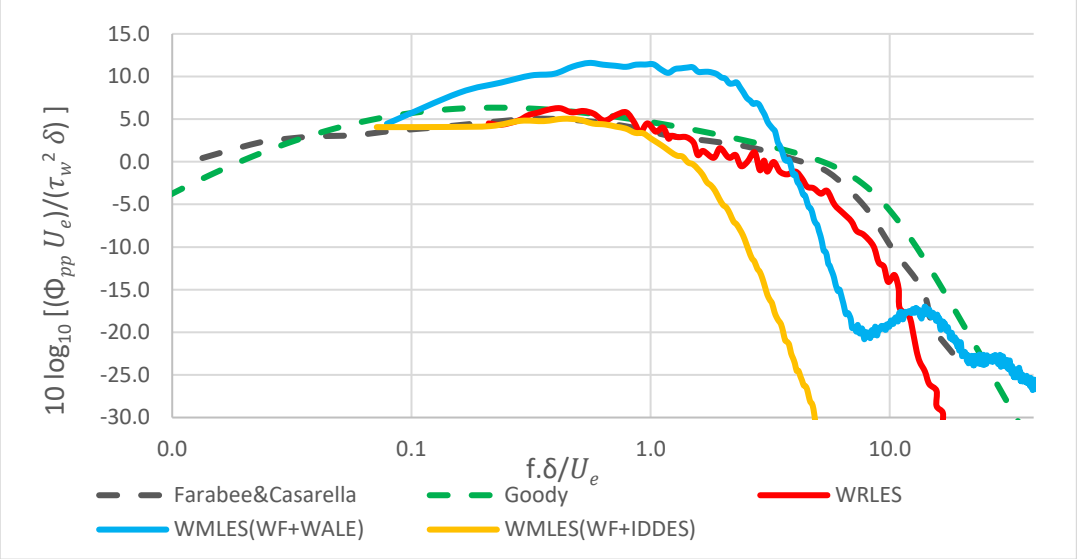

Figure 1: Power spectral density of pressure fluctuations in channel flow at Re_τ= 2000, plotted using mixed inner/outer scaling. Comparison of LES methods with experimental data [4] and an empirical correlation [5].

References

[1] M.L Shur, P.R Spalart, M.K Strelets, A.K.Travin, "A hybrid RANS-LES approach with delayed-DES and wall-modeled LES capabilities", *Int. J. Heat Fluid Flow*, **29**, 1638–1649, 2008.

[2] M. Liefvendahl, G. Lane, M. Winroth, P. Croaker, "Wall-pressure fluctuations from wall-modelled large-eddy simulations", *34th Symposium on Naval Hydrodynamics*, Washington, DC, USA, 26 June – 1 July, 2022.

[3] G. Grasso, P. Jaiswal, H. Wu, S. Moreau, M. Roger, "Analytical models of the wall-pressure spectrum under a turbulent boundary layer with adverse pressure gradient", *J. Fluid Mech.*, **877**:1000–1062, 2019.

[4] T.M. Farabee, M.J. Casarella, "Spectral features of wall pressure fluctuations beneath turbulent boundary layers", *Phys. Fluids A*, **3**, 2410–2420, 1991.

[5] M. Goody, "Empirical spectral model of surface pressure fluctuations", *AIAA J.*, **42**(9):1788–1794, 2004.

Broadband noise predictions using large eddy simulations: further analysis of boundary layer statistics

Thomas Lloyd[1], Artur Lidtke[1], Maarten Kerkvliet[1], and Johan Bosschers[1]

[1]Maritime Research Institute Netherlands
Haagsteeg 2, Wageningen, 6700 AA, the Netherlands.
e-mail: {t.lloyd; a.lidtke; m.kerkvliet; j.bosschers}@marin.nl

Signature and self-noise are important in the design of naval vessels, requiring reliable prediction methods for flow noise. Broadband noise predictions at low Mach numbers can be made using acoustic analogies or semi-analytical noise models, with the necessary input quantities derived from incompressible computational fluid dynamics (CFD) simulations. This avoids the need for more expensive compressible Navier-Stokes and/or Euler equation simulations of the sound generation and propagation. Applications of semi-empirical noise models involving both Reynolds-averaged Navier-Stokes (RANS) simulations and scale-resolving simulations (SRS) can be found in the literature [1].

In our recent paper [2] we presented a comparison of far-field noise predictions using several semi-analytical trailing edge noise models, with the input quantities obtained from large eddy simulations (LES). The comparison error of each prediction against measurement data was shown to be strongly dependent on the type of input data required and the associated errors in the incompressible hydrodynamic flow solution. This is highlighted in Figure 1b for predictions made using Amiet's trailing edge noise model [3], which requires a turbulent wall pressure spectrum (shown in Figure 1a) and spanwise coherence length scale as input. It was hypothesised that the observed differences are related to numerical errors in the LES results, potentially originating from how boundary layer transition to turbulence was handled in the simulations, with the resulting flow features convected to the trailing edge. Further analysis of the boundary layer development along the aerofoil chord is required to confirm this.

In this new study we analyse the effect of numerical errors on semi-analytical predictions in more detail by simulating a flat plate using LES, following the setup reported in [4]. Transition is induced by a zig-zag trip included in the computational domain (whereas a step trip was used in [2]). The development of the turbulent boundary layer for this case is visualised using the axial skin friction coefficient in Figure 2. Analysis of the turbulent boundary layer along the plate will focus on the quantities relevant for semi-analytical noise predictions, including the turbulent wall pressure spectra and spanwise coherence length. Furthermore, additional semi-analytical models which were not previously considered in [2] will be evaluated.

References

[1] M. Herr, R. Ewert, C. Rautmann, M. Kamruzzaman, D. Bekiropoulos, A. Iob, R. Arina, P. Batten, S. Chakravarthy, and F. Bertagnolio, "Broadband trailing-edge noise predictions— overview of BANC-III results," *21st AIAA/CEAS Aeroacoustics Conference*, 2015.

[2] T. Lloyd, A. Lidtke, M. Kerkvliet, and J. Bosschers, "Broadband trailing-edge noise predictions using incompressible large eddy simulations," in *28th AIAA/CEAS Aeroacoustics 2022 Conference*, (14th-17th June, Southampton, UK), American Institute of Aeronautics and Astronautics, 2022.

[3] R. Amiet, "Noise due to turbulent flow past a trailing edge," *Journal of Sound and Vibration*, vol. 47, no. 3, pp. 387–393, 1976.

[4] W. C. Van Der Velden, A. H. Van Zuijlen, A. T. De Jong, and D. Ragni, "Flow and self-noise around bypass transition strips," *Noise Control Engineering Journal*, vol. 65, no. 5, pp. 434–445, 2017.

[5] A. S. H. Lau, J. W. Kim, J. Hurault, and T. Vronsky, "A study on the prediction of aerofoil trailing-edge noise for wind-turbine applications," *Wind Energy*, vol. 20, no. 2, pp. 233–252, 2017.

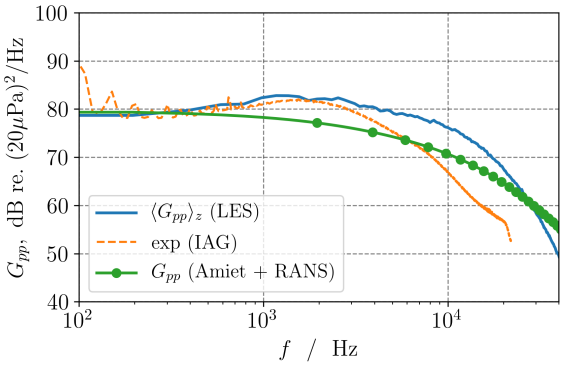

(a) Turbulent wall pressure spectra at the trailing edge predicted by LES and Amiet empirical model, compared to measurement data.

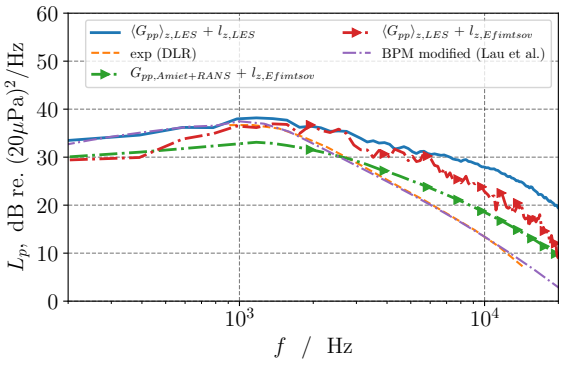

(b) Far-field sound pressure level spectra predicted using Amiet's trailing edge noise model with several different sources of input data, compared to measurement data and empirical model [5].

Figure 1: Noise predictions from viscous CFD simulations of the turbulent flow over a NACA 0012 aerofoil [2].

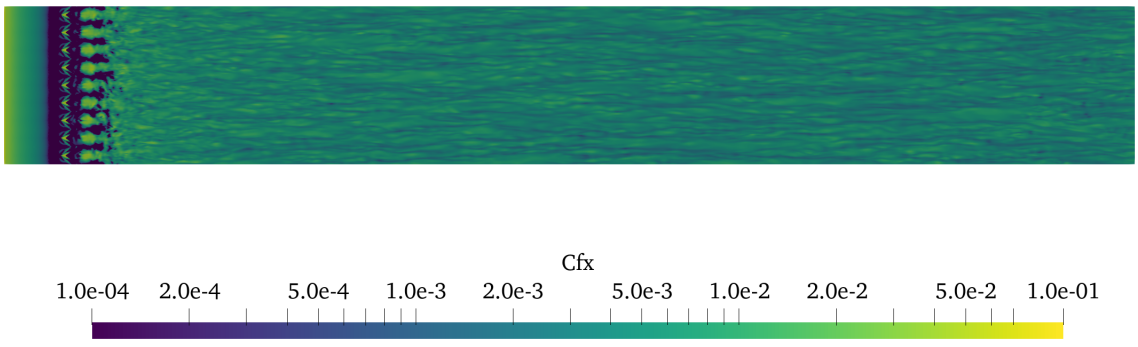

Figure 2: Instantaneous streamwise component of skin friction coefficient over flat plate simulated using LES. Flow is from left to right with zig-zag trip located at $0.1c$.

Study of Flow Noise with a Buoyancy-Driven Model

Ian MacGillivray[1], Daniel Lamos[1], Jeff Seers[1], and Alex Skvortsov[1]

[1]Platforms Division, Defence Science and Technology
Melbourne, Victoria 3027, Australia
e-mail: ian.macgillivray@defence.gov.au

Flow noise phenomena are often related to background acoustic noise of the atmosphere and ocean, and anthropogenic noise pollution such as noise generated by aircraft and maritime vehicles. Flow noise is very difficult to study experimentally, because it is often very weak (at least for small-scale models) and can be masked by extraneous noise entering or generated by the experimental facility (e.g. flow conditioning devices, fan motors, lab stand vibration, etc.) preventing its reliable identification and estimation. These factors make any laboratory study of flow noise a rather difficult and often expensive undertaking involving complex experimental facilities.

Extending our previous work [1, 2], we present a study of a cost-effective experimental investigation of flow noise measurement with a small-scale buoyancy driven model (BDM). The specific aim of the investigation is to obtain accurate measurements of total radiated sound power as well as sound power radiated in specific directions. For a test case we evaluate a BDM (approximately 0.9 m in length) operating in DST Group's Large Water Tank, which has a length, width and depth of 10 m $\times$ 10 m $\times$ 6 m, respectively. The tank functions as a highly reverberant space, and standard room-acoustic methods can be used to measure the total radiated power in fractional-octave bands from sources within the tank, based on the tank reverberation times. Our typical BDM can reach a speed of order 7 m/s, close to terminal velocity, within about 0.7 secondsnts of the BDM velocity, and internal accelerometer measurements, are combined to quantify the BDM characteristics such as added mass and drag coefficient, and thus the achievable terminal velocity.

Although the water tank is reverberant, the high speed of sound in water combined with relatively short T_{60} reverberation times of order 1 second above about 1 kHz means that the instantaneous sound power is closely approximated by the reverberant power at each time even though the reverberant power lags the flow noise power because of the time required for reverberant build-up. Nevertheless, using knowledge of the velocity versus time and an assumed power dependence to the radiated power, the measured power can be corrected for this small effect.

Because of the short run time of a BDM in our tank it is critical that all possible noises associated with the release of the BDM are reduced to a minimum. Most mechanical noises can be satisfactorily reduced, but one issue yet to be satisfactorily resolved concerns the release noise associated with the 'step' change of force that acts on both the BDM and the release-support structure. Simple estimates of the magnitude of this noise at the frequencies of interest for an abrupt force release put the noise at a level comparable or greater than the expected flow noise. Initial measurements have confirmed this. For a neutrally buoyant BDM (which would not actually be a BDM!) any force step change would result in radiated power corresponding to the standard force dipole. The radiated power is directly related to the 'instantaneous' acceleration of the structure when the force is released, and for BDM structures of density different to the surrounding fluid the radiated power is different. For a very light structure the power can be increased significantly, especially if the added mass relative to the displaced mass of the slender BDM is small. Conversely, if we consider a 'ballast' driven model with density much greater than water then the radiated power caused by the force

step change is reduced in rough proportion to the ratio of the fluid mass to the model mass. With a steel model reductions of order 20 dB should be achievable. Consequently, it is planned to present measurements of some initial trials with a heavy ballast driven model. For the buoyancy driven model itself it is planned to produce a release mechanism that smears the force step change to lower the higher frequency content.

Figure 1 presents initial results of total radiated one-third-octave band (OTOB) noise from the BDM, including the corrections required to convert the raw hydrophone measurements into total radiated power expressed as an equivalent spherical sound pressure level. The advantage of the reverberant tank is the ability to determine total radiated power. We will also be considering the deployment of array systems to both localise and directly measure the radiated power in specific directions using beamforming techniques.

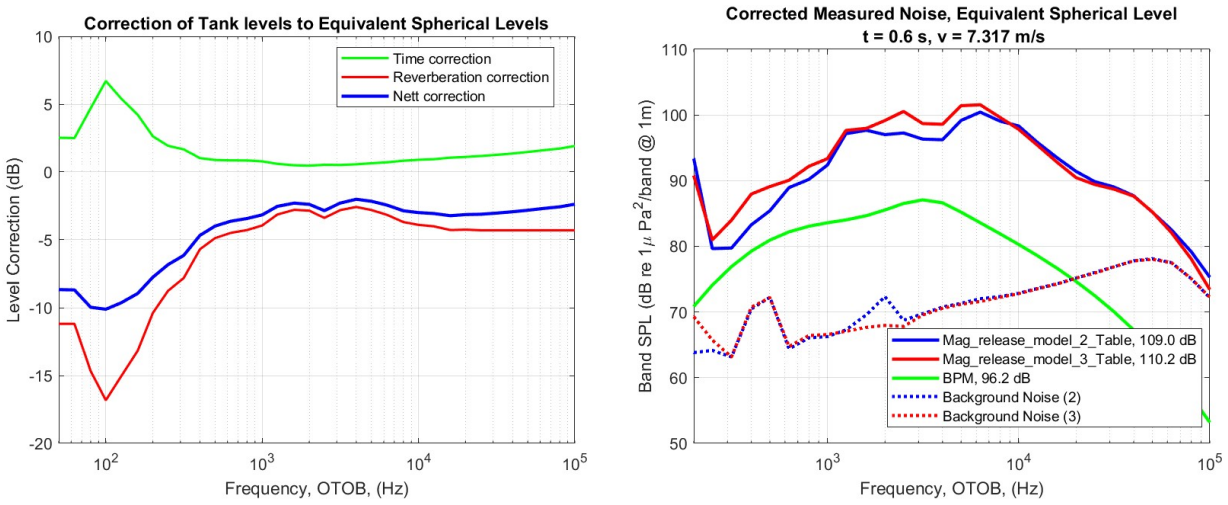

(a) (b)

Figure 1: (a) Level corrections required to convert measured reverberant levels in the tank into equivalent spherical source levels at 1 metre. Correction due to the time delay in reverberent build up (green curve), the reverberation-to-power correction from room acoustics theory based on T_{60} (red), and the net correction (blue). (b) Two preliminary measurements of a 0.9-m-long BDM travelling at 7.3 m/s (blue and red solid curves). The noise floor of the measurements (dashed) is predominantly equipment-limited above 3 kHz. The expected contribution to the noise from the BDM's 4 aft NACAA 12 hydrofoils (dimensions 0.1 m $\times$ 0.1 m) from BPM-based predictions [3] when scaled to water.

References

[1] J. Fischer, C. Doolan, M. Rowan, D. Lamos, J. Seers, O. Vargas, S. Lam, and A. Skvortsov, "Acoustic localization of a buoyancy driven model using a beamforming hydrophone array," *Applied Acoustics*, vol. 174, no. 107798, 2021. doi:10.1016/j.apacoust.2020.107798.

[2] J. Yen, D. Butler, D. Lamos, J. Seers, D. Clarke, R. Cairns, M. Rowan, and A. Skvortsov, "Experiments and simulations of an accelerating buoyancy-driven model," in *21st Australasian Fluid Mechanics Conference, Adelaide, Australia*, 10-13 Dec 2018.

[3] T. F. Brooks, D. S. Pope, and M. A. Marcolini, "Airfoil self noise and prediction," Tech. Rep. NASA Reference Publication 1218, NASA, 1989.

Modelling and characterization of micro-porous resonating liners under a low speed flow

Cédric Maury[1], Teresa Bravo[2] and Daniel Mazzoni[3]

[1]Aix Marseille Univ. CNRS Centrale Marseille, Laboratory of Mechanics and Acoustics (LMA UMR 7031)
38 rue Frédéric Joliot-Curie, 13013 Marseille, France
cedric.maury@centrale-marseille.fr

[2]Instituto de Tecnologías Físicas y de la Información (ITEFI), Consejo Superior de Investigaciones Científicas (CSIC)
Serrano 144, 28006 Madrid, Spain
teresa.bravo@csic.es

[3] Aix Marseille Univ. CNRS Centrale Marseille, Institut de Recherche sur les Phénomènes Hors Equilibres (IRPHE UMR 7342)
38 rue Frédéric Joliot-Curie, 13013 Marseille, France
daniel.mazzoni@centrale-marseille.fr

Enhancing the dissipation of low-frequency noise components in low-speed ducted flows is of paramount importance for the mitigation of exhaust pipes emissions in the automotive sector, but also to decrease the sound radiated by HVAC (Heat, Ventilating and Air Conditioning) diffusers towards residential areas. Typical resonant silencers such as expansion chambers, Helmholtz resonators or locally-reacting perforated liners are able to achieve high acoustical performance over a targeted bandwidth. But they also have to cope with aerodynamic constraints such as low frictional losses or minimal pressure drop [1] or to overcome aero-acoustic adverse conditions due to the generation of flow-silencer interaction noise, coined flow-induced noise, that impede the acoustical attenuation performance [2].

The current study evaluates the aero-acoustic efficiency of axially-graded resonating liners with micro-porous interface under a low-speed flow. The idea is to generate slow-sound effects from a distribution of varying cavity depths in order to trap and fully dissipate the incident acoustic wave over a specific bandwidth due to visco-thermal effects. Such concept has essentially been developed in the no-flow case assuming closed-end conditions [3]. The micro-porous interface aims at shielding the liner from the flow effects to avoid flow-induced noise, but also to enhance the dissipated power and achieve minimal pressure drop. These issues will be studied from theoretical, numerical and experimental approaches.

Analytical models are considered based on the transfer matrix formulation assuming a plug flow and micro-perforated wall impedances identified from duct flow measurements up to a Mach number of 0.15 [4]. The indicators will be the reflected power, the transmission loss, the dissipated power and the axial variations of the acoustic field within the axially-graded silencer. Due to the wave trapping phenomenon, both the transmitted and reflected waves will drop to zero over a specific bandwidth, the so-called Acoustic Black Hole (ABH) effect.

A key issue is the robustness of the ABH effect to realistic low-speed flow conditions. It will be examined from numerical models of acoustic wave propagation in a ducted flow lined by the ABH silencer. A Large Eddy Simulation (LES) model of a compressible low-speed turbulent flow will be implemented with special focus on the interaction between the flow and the silencer ring cavities. In particular, the balance between flow-induced noise generation and visco-thermal dissipation in wall cavities at specific frequencies will be examined [see Fig. 1(left)]. The influence of a micro-porous cavity-flow interface will be scrutinized locally, but also globally to assess its effect on the acoustical

properties of the ABH silencer. Experimental verification of the simulated ABH silencer aeroacoustic performance will be carried out on a low-speed flow wind-tunnel shown in Fig. 1(right). The test rig enables measurement of the scattering matrix properties of the ABH silencer section from in-flow pressure measurements using nosecone microphones located apart from the test section and a two-source method. Guidelines will be provided on the geometrical parameters of axially-graded resonating silencers and their interface to achieve ABH effect over a targeted frequency bandwidth for given flow conditions.

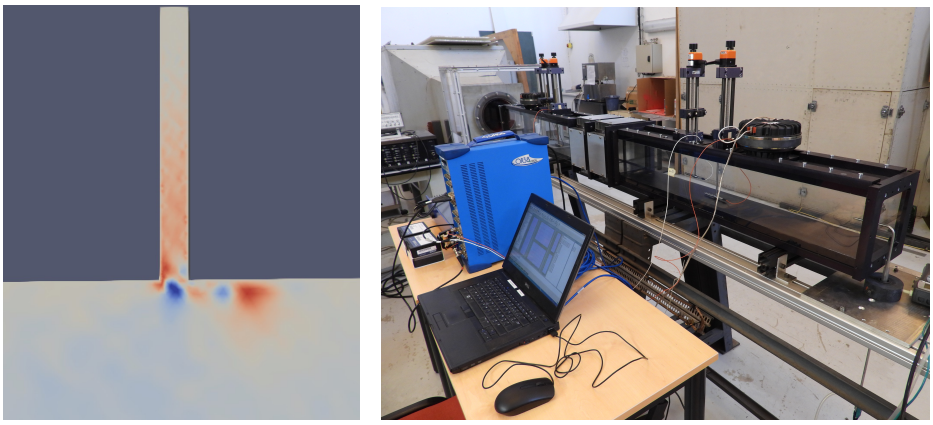

Figure 1: (left) LES simulation (OpenFOAM) of flow-cavity interaction effects between a low-speed turbulent flow at Mach 0.1 and a non-resonating cavity, part of the ABH silencer; (right) aeroacoustic test rig for measurement of the scattering matrix properties of silencers under a low-speed turbulent flow using the two-source method.

References

[1] B. M. Howerton, M. J. Jones 2016 Acoustic liner drag: measurements on novel facesheet perforate geometries, in: *Proceedings of the 16th AIAA/CEAS Aeroacoustics Conference*, Lyon, AIAA paper 2016-2979.

[2] C. Maury, T. Bravo, D. Mazzoni 2021 Absorption and transmission of boundary layer noise through micro-perforated structures: measurements and modellings, in *FLINOVIA - Flow-Induced Noise and Vibrations Issues and Aspects - III.* Ciappi**,** E., De Rosa, S., Franco, F., Hambric, S.A., Leung**,** R.C.K., Clair, V., Maxit, L., Totaro, N. (Eds.), Springer Nature, Switzerland.

[3] Y. Mi, W. Zhai, L. Cheng, C. Xi, X. Yu 2021 Wave trapping by acoustic black hole: Simultaneous reduction of sound reflection and transmission, *Applied Physics Letters* 118 114101.

[4] C. Maury, T. Bravo and D. Mazzoni 2019 The use of microperforations to attenuate the cavity pressure fluctuations induced by a low-speed flow, *Journal of Sound and Vibration*, vol. 439, pp. 1-16.

Investigations about the experimental application of PEDEm for the reproduction of a structural response to a Turbulent Boundary Layer excitation

Giulia Mazzeo[1], Mohamed N. Ichchou[1], Giuseppe Petrone[2], Olivier Bareille[1], Francesco Franco[2], and Sergio De Rosa[2]

[1]LTDS — Laboratoire de Tribologie et Dynamique des Systèmes, Ecole Centrale de Lyon
Ecully 69130, France
e-mail: giulia.mazzeo@ec-lyon.fr, mohamed.ichchou@ec-lyon.fr, olivier.bareille@ec-lyon.fr
[2]PASTA LAB — Laboratory for Promoting Experiences in Aeronautical Structures and Acoustics, University "Federico II" of Naples
Naples 80125, Italy
e-mail: giulia.mazzeo@unina.it, giuseppe.petrone@unina.it, sergio.derosa@unina.it, francesco.franco@unina.it

The vibrational response of a structure subjected to Wall-Pressure Fluctuations (WPFs) due to a turbulent flow is one of the major problems still being addressed in transportation fields as automotive, railway, naval and aeronautics. Consequences of Turbulent Boundary Layer (TBL) induced vibrations might be several: the external surfaces of any vehicle can exhibit fatigue problems and structural damages due to the flow-induced vibrations; the payload or any good transported by a vehicle can be damaged because the interior induced vibrations exceed the design requirements; the TBL excitation is a source of air-borne sound and it influences a structure-borne sound to any vehicle, generating discomfort for passengers and noise pollution in the environment. These are just few reasons for which the study of TBL-induced vibrations is of critical importance in both academic and industrial fields.

Until today, wind tunnels are the most used facilities for recreating the physical condition of a TBL excitation over a structure; indeed, they can be exploited to measure the vibrational response of simple structures, e.g. panels, subjected to an aerodynamic load. Several issues can be encountered during the performance of this type of experiments in a wind tunnel. As the sample panel is mounted inside the test section of the facility, the acquired measurements can be compromised because of the background noise of the drive system or due to the induced vibrations of the sample support. In general, experiments in a wind tunnel are not efficiently performed due to technical complications and they can be expensive in both economical and time-consuming sense.

To overcome the aforementioned issues, alternative methodologies have been proposed recently. They all consist in approximating the TBL spatial distribution as an uncorrelated pressure field in a high frequency domain. Experimentally, they rely on the implementation of loudspeakers [1] or shakers [2] to excite the structure in different positions; then, the measured data are post-processed in order to obtain the equivalent vibrational response of the structure as it is subjected to a TBL excitation. Recently, a similar work has been proposed by the authors, taking as a reference methodology the Pseudo-Equivalent Deterministic Excitation method (PEDEm) [3] and applying it for experimental purposes [4]. It has been numerically demonstrated that by choosing in a random way a selection of acquisition points and excitation points, it is possible to reproduce the vibrational response of a panel subjected to a TBL excitation in two different boundary conditions (simply-supported and clamped). The method, called Experimental PEDEm (X-PEDEm) rely on the application of several deterministic forces through a hammer test and it ensure a high versatility for the

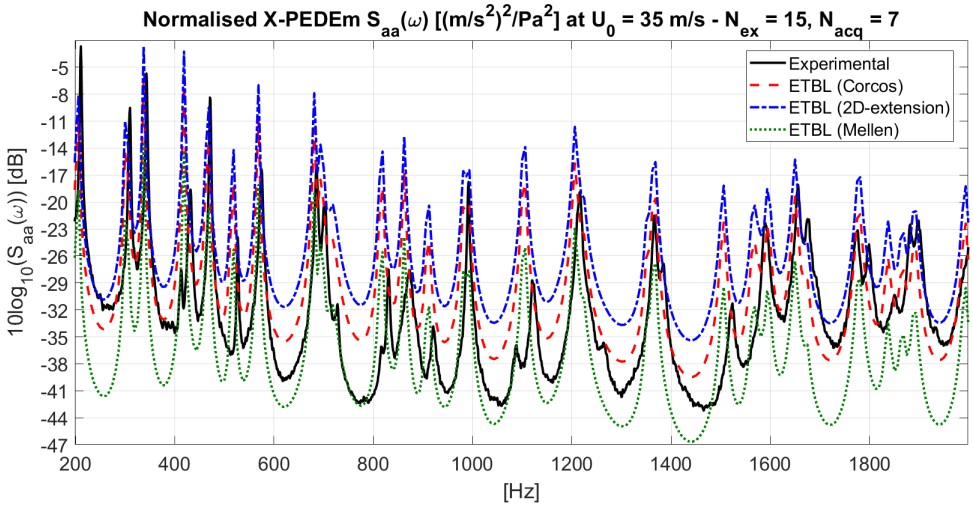

Figure 1: Experimental acceleration PSD of an aluminium panel collected in a wind tunnel ($U_0 = 80$ m/s), in comparison with X-PEDEm, over 7 acquisition points and 15 excitation points. (solid black line) experimental, (dashed red line) X-PEDEm calculated with ETBL based on Corcos model, (dashed-dotted blue line) X-PEDEm calculated with ETBL 2D-extension model, (dotted green line) X-PEDEm calculated with ETBL based on Mellen model.

post-processing of the measured data: three different Equivalent TBL (ETBL) models have been introduced in the method (Figure 1), and both numerical or experimental coefficients for the TBL description can be equivalently implemented. In this work, it is wanted to validate X-PEDEm by comparing the experimental vibrational response of a plate measured through a hammer test with the numerical response of a plate subjected to a TBL excitation. Different TBL models, together with different boundary conditions will be taken into account in order to validate the versatility of the experimental method. A comparison between the experimental X-PEDEm and the experimental results obtained in a wind tunnel will be considered too. Finally, it is wanted to investigate the conditions for which it is possible to extend the X-PEDEm method to the low frequency domain, where the spatial distribution of the TBL wall-pressure field is no more uncorrelated, in order to ensure a broadband frequency range of application of the methodology.

References

[1] L. Maxit, "Simulation of the pressure field beneath a turbulent boundary layer using realizations of uncorrelated wall plane waves," *The Journal of the Acoustical Society of America*, vol. 140, no. 2, pp. 1268–1285, 2016.

[2] T. Bravo and C. Maury, "A synthesis approach for reproducing the response of aircraft panels to a turbulent boundary layer excitation," *The Journal of the Acoustical Society of America*, vol. 129, no. 1, pp. 143–153, 2011.

[3] S. D. Rosa, F. Franco, and E. Ciappi, "A simplified method for the analysis of the stochastic response in discrete coordinates," *Journal of Sound and Vibration*, vol. 339, pp. 359–375, 2015.

[4] G. Mazzeo, M. Ichchou, G. Petrone, O. Bareille, S. D. Rosa, and F. Franco, "Pseudo-equivalent deterministic excitation method application for experimental reproduction of a structural response to a turbulent boundary layer excitation," *The Journal of the Acoustical Society of America*, vol. 152, no. 3, pp. 1498–1514, 2022.

Mitigation of Cavity Noise with Aeroacoustically Excited Surface Panels

Muhammad Rehan Naseer[1], Muhammad Irsalan Arif[2] and Randolph C. K. Leung[3]

Department of Mechanical Engineering, The Hong Kong Polytechnic University,
Kowloon, Hong Kong, People's Republic of China

Email: [1]rehan.naseer@connect.polyu.hk; [2]irsalan.arif@connect.polyu.hk; [3]mmrleung@polyu.edu.hk

The suppression of deep cavity tonal noise has been an alluring area of aeroacoustic research due to its application in a wide range of mechanical systems, such as closed side branches in gas transport systems, turbomachineries and safety valves. Over the period, numerous cavity noise reduction techniques have been developed and evaluated [1-4], which involved modifying shapes of leading and trailing edges, installing plasma actuators and leading edge blow system. However, the implementation of these strategies is limited by the overriding concerns, firstly the requirement of significant geometrical redesigning challenges the practicality of such system, secondly the idea of eventual perturbation of the shear layer to evade the Rossiter mode comes with the inevitable penalty of additive drag apart from completely changing the cavity flow regime.

A novel approach for reducing cavity tonal noise using flow-induced surface vibrations is investigated in this study by utilizing an elastic panel flush-mounted at the cavity bottom wall. The main goal of this current exercise is to reduce the tonal noise while maintaining the shear layer over the cavity opening characteristically same with little or no adverse effects on the aerodynamic performance of the cavity. The two-way aeroacoustic-structural interaction of the designed elastic panel modifies the phase and intensity of the incident acoustic waves inside the cavity which subsequently modifies the receptivity pattern of the aeroacoustic coupling at the cavity leading edge and eventually results in reduction of tonal noise. A uniform flow with Mach number, $M = 0.09$ and Reynolds number, $Re = 4\times10^4$ passing over a deep cavity of an aspect ratio, $L/D = 0.25$ is chosen as baseline rigid cavity case (*RC*) due to its extensive experimental information available in the existing literature. Concerning the complexity of the subject problem, Direct Aeroacoustics Simulation (DAS) is employed to solve the unsteady compressible N-S equations using the Conservation Element and Solution Element (CE/SE) method while one dimensional plate equation is used to cater the nonlinear dynamic response of the elastic panel.

A flush-mounted elastic panel replaces the bottom wall of the cavity (*EP*) to analyze the envisaged mechanism of aeroacoustic-structural interaction and the vibrational response of the panel in suppressing the deep cavity tonal noise. The choice of panel mounting location is guided by the baseline *RC* case, which indicates that the depth of the cavity is exposed to purely acoustic fluctuations, thereby abating them could shift the acoustic phase out of sync with the shear layer oscillation to achieve noise reduction. Panel parameters such as internal tension, thickness, and density are carefully designed to ensure that the natural frequency of the panel is similar to the first dominated frequency of the cavity flow field so that a resonance condition is achieved for the effective transmission of the perturbation energy into the sustained panel vibration.

Investigation revealed a noticeable reduction in the magnitude of pressure fluctuations across the bottom region for cavity with an elastic panel. Furthermore, a significant reduction in pressure fluctuations around the cavity is also observed. A comparison of sound pressure level with the baseline rigid cavity showed promising reduction in tonal noise of cavity-panel configuration by 3.6 dB as shown in Fig. 1. Further, the cavity leading edge phase information reveals a modified phase pattern for *EP* compared to *RC*, where a strongly coupled shear layer oscillation produces intense acoustic emission, contrary to the modified interaction in the case of *EP*, which results in weaker noise radiation.

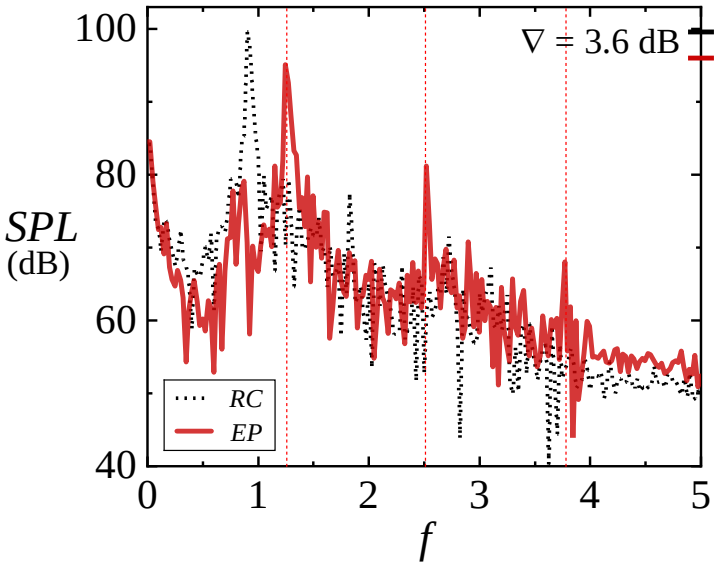

Figure 1. SPL spectrum of *RC* and *EP* configurations calculated at (*x*, *y*)=(6.75, 21.5) from cavity leading edge.

Acknowledgments

The authors gratefully acknowledge the support from the Research Grants Council of the Government of Hong Kong Special Administrative Region under grant number 15208520. The first author is grateful to stipend support to his study from the Department of Mechanical Engineering, The Hong Kong Polytechnic University.

References

[1] L. N. Cattafesta III, Q. Song, D. R. Williams, C. W. Rowley, and F. S. Alvi, "Active control of flow-induced cavity oscillations," *Progress in Aerospace Sciences*, vol. 44, no. 7-8, pp. 479-502, 2008.

[2] D. G. MacManus and D. S. Doran, "Passive control of transonic cavity flow," *Journal of Fluids Engineering*, vol. 130, no. 6, 2008.

[3] S. Lawson and G. Barakos, "Review of numerical simulations for high-speed, turbulent cavity flows," *Progress in Aerospace Sciences*, vol. 47, no. 3, pp. 186-216, 2011.

[4] A. J. Saddington, V. Thangamani, and K. Knowles, "Comparison of passive flow control methods for a cavity in transonic flow," *Journal of Aircraft*, vol. 53, no. 5, pp. 1439-1447, 2016.

Similitude Laws for Scaling Vibrations and Acoustic Radiation of Panels Excited by a Turbulent Boundary Layer

Xavier Plouseau-Guédé[1,2,3], Alain Berry[1], Laurent Maxit[2], and Valentin Meyer[3]

[1]Groupe d'Acoustique de l'Université de Sherbrooke (GAUS), Université de Sherbrooke,
Sherbrooke, QC J1K 2R1, Canada
e-mail: xavier.plouseau-guede@usherbrooke.ca
e-mail: alain.berry@usherbrooke.ca
[2]Univ Lyon, INSA Lyon, Laboratoire Vibrations-Acoustique (LVA),
25 bis av. Jean Capelle, 69610, Villeurbanne Cedex, France
e-mail: laurent.maxit@insa-lyon.fr
[3]Naval Group Research,
199 av. Pierre Gilles de Gennes, 83190, Ollioules, France
e-mail: valentin.meyer@naval-group.com

This study is related to noise control in the transport industry, such as aeronautics, rail, automotive or naval. In particular, this paper focuses on the noise radiated by structures excited by turbulent flows induced by the movement of an underwater vehicle. This excitation is due to the pressure and velocity fluctuations within the Turbulent Boundary Layer (TBL). These wall pressure fluctuations generate vibrations as well as acoustic radiation in water. The vibroacoustic behavior of the underwater vehicle needs to be controlled in order to ensure high operational performances with regards to radiated noise and sonar performances. However, the numerical simulations of the hydro-vibro-acoustic problem are very complex and costly in terms of calculation time for industrial applications. In addition, experiments on underwater vehicles are costly, time-consuming and difficult to implement. These experiments cannot be carried out during preliminary project phases for new vehicles, such as submarines or surface ships (see Figure 1, left). Therefore, reduced scale models (see Figure 1, right) can be used to design underwater vehicles with improved acoustic performances. Similitude laws have been developed in the past for different fields of physics, such as hydrodynamics, but have only recently been applied to vibroacoustics. The question raised in this paper is to know whether the vibroacoustic behavior of two systems can be linked through similitude laws in the case of a TBL excitation and heavy fluid loading.

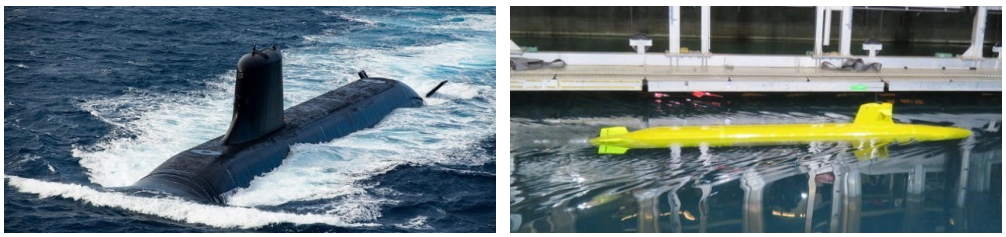

Figure 1: (left) Picture of an operational submarine, (right) submarine model in a measuring tank.

This approach consists in linking the properties of two systems (materials, fluids, dimensions, loading conditions) so that the response of one system can be estimated by scaling the response of the other. From measurements carried out on a model of an underwater vehicle, the noise radiated by the full-scale vehicle

is predicted by applying the similitude laws developed using the similitude theory. Recent work in the field of vibroacoustic similitude laws applied to simple systems (for plates see [1]) has advanced the similitude theory and shown its importance. Especially, similitude laws have been proposed for plates in air excited by a TBL and validated experimentally [2, 3]. However, the analysis have been limited to the vibrations of the structure and the acoustic radiation has not been addressed.

In the present study, similitude laws for the vibration and the acoustic radiation of thin plates excited by a TBL are developed. The considered plates are supposed of constant thickness and made of an isotropic elastic material and having the same boundary conditions. Here, they have simply supported boundary conditions on their four edges. The TBL is considered homogeneous, stationary and fully developed. The similitude laws concern the vibratory response (spatially-averaged squared velocity and local velocity) and the acoustic response (radiated pressure, sound power). Two aspects are particularly studied, detailed as follows :

- The strong coupling between the structure and the surrounding heavy fluid. Contrary to a structure vibrating in air, the influence of water on the structure vibrations is no longer negligible. This implies to satisfy specific similitude conditions, as demonstrated in [4] for fluid-loaded plates excited by a point force. This result is extended for plates excited by a TBL. From an analytical model of a submerged plate, similitude conditions are established in order to obtain exact similitude laws. These similitude conditions allow to determine the properties of the scaled plate and the scaled fluid. Several numerical examples, in air and in water, are presented to illustrate and validate the vibroacoustic similitude laws.

- The experimental validation of the similitude law for the sound power of plates in air excited by a TBL. After a numerical verification, it has to be experimentally validated. However, only few experimental results exist in the literature for the acoustic radiation of panels excited by a TBL. Hence, a measurement campaign was carried out in an anechoic wind tunnel at the University of Sherbrooke to characterize the radiation of different plates and for different flow velocities. Particular attention was given to the estimation of the power radiated by the plate under this low-level random excitation.

References

[1] A. Casaburo, G. Petrone, F. Franco, and S. De Rosa, "Similitude theory applied to plates in vibroacoustic field: a review up to 2020," *Progress in Scale Modeling*, 2020. Publisher: University of Kentucky.

[2] O. Robin, F. Franco, S. De Rosa, E. Ciappi, and A. Berry, "Scaling laws for flat plate vibroacoustic response induced by a deterministic and random excitations," in *Noise and Vibration Emerging Methods*, (Ibiza, Spain), 2018.

[3] F. Franco, O. Robin, E. Ciappi, S. De Rosa, A. Berry, and G. Petrone, "Similitude laws for the structural response of flat plates under a turbulent boundary layer excitation," *Mechanical Systems and Signal Processing*, vol. 129, pp. 590–613, 2019.

[4] X. Plouseau-Guédé, A. Berry, L. Maxit, and V. Meyer, "Vibroacoustic similitude laws for fluid-loaded plates excited by point forces," in *International Congress on Sound and Vibration*, (Singapore), 2022.

Acoustic Measurements of Multiphase Tip-Leakage Flow.

Patrick S. Russell, Luka Barbaca, James Venning, Bryce Pearce, and Paul Brandner.

Cavitation Research Laboratory, The University of Tasmania
Building A1, Maritime Way, TAS 7250, Australia
Email: patrick.russell@utas.edu.au

Efforts to understand cavitation in tip-leakage flow have been renewed after recent findings on the nature of inception in these flows. A liquid may locally come under tension due to the strong pressure drop at the core of a vortex. Pure liquids can often sustain these high negative pressures. However, should tension coincide with the presence of a suitable nucleus (such as a gas bubble) cavitation inside the vortex will form. Such cavitation often occurs in vortices shed from lifting surfaces or in a turbulent shear flow. In shear flows the activation of a specific nuclei is an unlikely event, as the trajectory and pressure it will experience are probabilistic [1]. This likelihood may improve when a vortex retains a coherent structure, drawing bubbles into its core through buoyancy. However, recent studies have shown that inception often first occurs when a smaller vortex is rapidly stretched around a larger structure [2]. Stretching of a vortex produces necking along the axis of the vortex core increasing circulation and reducing its radius to produce a spike in low pressure. Flow escaping from the tip-clearance of pumps, ducted propulsors and turbomachinery readily provides such conditions, as they are typified by a strong primary vortex composed of many co-rotating sub-vortices and a plethora of sources for weaker secondary vortical structures [3], all rolling up to capture nuclei from a large cross-section of the flow [4]. Inception in these flows is usually established through acoustic measurements. Incipient and developed vortex cavitation bubbles can exhibit complex dynamics as the bubble interacts with the surrounding flow. The growth, deformation, fragmentation, and collapse of the cavity can lead to narrow or broadband sound emissions, see Figure 1. Although acoustic spectra may indicate increased power at select frequencies, the small incipient structures that signal inception may spread their minimal energy over a range of frequencies. Wavelet analysis can help identify the frequencies of interest and assist in development of subsequent less-expensive methods of detection. These processes are used investigate the effect of nuclei size and concentration on the inception of cavitation in tip leakage flow for a range of incidence and clearance ratios (gap height normalized by the maximum thickness of the hydrofoil). While trends with gap height and incidence remain similar, the presence of weaker nuclei require less tension for cavitation to incept.

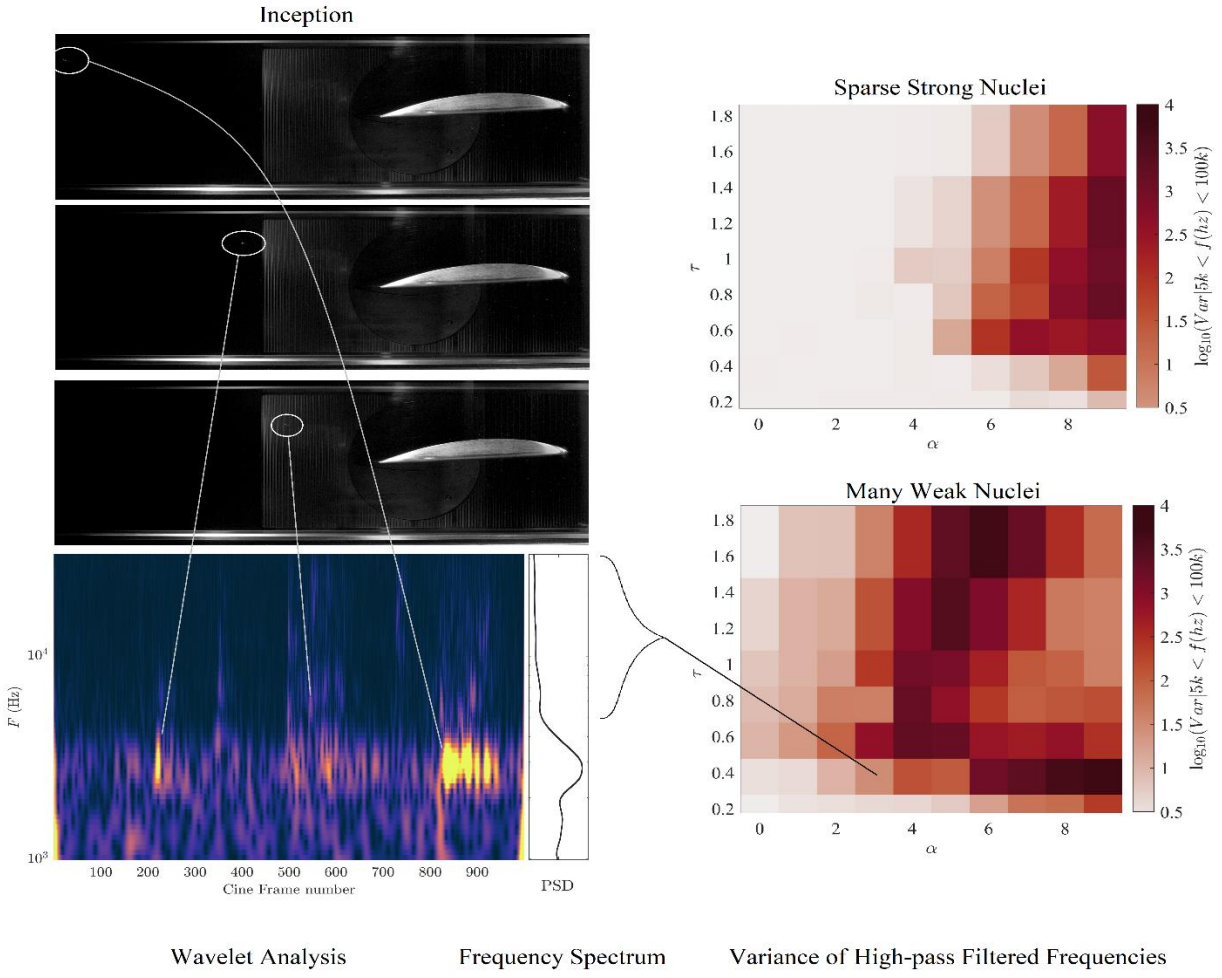

Figure 1: Simultaneous acoustic and highspeed photographic measurement of cavitation in tip leakage flow are presented. Images of three incipient events are shown. Also plotted is the continuous wavelet transform of the acoustic data including the time at which the images were sampled. The variance of the high-frequency component was calculated for a range of gap height $\tau = \frac{h}{max\ thickness}$ and incidence α. Additional fluctuations in the higher frequencies can be observed for a gap height of approximately $\tau = 0.6$.

References

[1] E. Allan, L. Barbaca, J. A. Venning, P. S. Russell, B. W. Pearce, and P. A. Brandner, "Nucleation and cavitation inception in high Reynolds number shear layers," *Physics of Fluids – under review* (2022).

[2] K. Agarwal, O. Ram, Y. Lu, and J. Katz, "On the Unsteady Pressure field, Nuclei Dynamics and Cavitation Inception in a Turbulent Shear Layer," in *Symposium on Naval Hydrodynamics*, 2022.

[3] G. F. Oweis, and S. L. Ceccio. "Instantaneous and time-averaged flow fields of multiple vortices in the tip region of a ducted propulsor." *Experiments in Fluids* 38, no. 5 (2005): 615-636.

[4] P. S. Russell, L. Barbaca, J. Venning, B. Pearce, and P. Brandner, "The influence of nucleation on cavitation inception in tip-leakage flows", *Physics of Fluids (accepted)*, 2022.

Wavenumber spectrum determination for transsonic wind tunnel measurements using FISTA

Carsten Spehr[1], Thomas Ahlefeldt[1], and Daniel Ernst[1]

[1]DLR German Aerospace Centre,
Bunsenstr 10, Goettingen, 37073, Germnay
e-mail: Carsten.Spehr@dlr.de, Thomas.Ahlefeldt@dlr.de, Daniel.Ernst@dlr.de

This paper deals with computational methods to determine the wavenumber spectrum of pressure fluctuation data measured by a phased sensor array underneath a transsonic boundary layer. The data are measured underneath a turbulent boundary layer of a flat plate in the transsonic wind tunnel Braunschweig with closed test section . The data were were previously published in 2012 using beamforming and a a so called embedded DAMAS2 deconvolution algorithm to obtain the wavenumber spectrum [1]. The aim of this paper is to re-post-processing these data with the newly introduced framework to find a well-defined unique solution with parametric L1 and L2 regularization.

The measurements were conducted in the Transonic-Wind-Tunnel Göttingen (TWG) a continously working wind tunnel with a cross section of 1 m x 1 m. A rigid flat plate with a length of about 2.75 m was mounted symmetrically in the closed test section. In the downstream part of the plate a sensor array with 48 piezo-resistive transduces is integrated using a threaded mounting.

For the entire analysis it is assumed that the correlation of pressure fluctuations p between two point $(x, y),\ (x', y')$ for a given frequency f can be described by a function that depends only on their spatial separation. We wish to reconstruct the frequency wavenumber spectrum at $(k_{n,x}, k_{n,y})$ for $n = 1, \dots N$, represented by a vector $\hat{\phi} \in \mathbb{C}^N$ with entries

$$\hat{\phi}_n = \widehat{\Phi}(k_{n,x}, k_{n,y}) \ . \tag{1}$$

An estimator of the discrete wavenumber spectrum can be obtained by the following regularized non-negative least squares problem

$$\min_{\hat{\phi} \geq 0} \frac{1}{2} \left\| \mathcal{T}(\hat{\phi}) - C^{\text{obs}} \right\|_F^2 + \frac{\alpha_2}{2} \left\| \hat{\phi} \right\|_2^2 + \alpha_1 \left\| \hat{\phi} \right\|_1 \ , \tag{2}$$

with regularization parameters α_1, α_2, the discrete forward model $C =: \mathcal{T}(\hat{\phi})$, where $C^{\text{obs}} \approx C$ is the noisy approximation of the (noise-free) data C (for any details see Raumer, Spehr [2]). The minimization problem from equation 2 was solved by the generalized FISTA algorithm (see [3]).

The top row in figure 1 shows the standard wavenumber maps (with DR) often called 'dirty' map. The bottom row shows the output of the FISTA algorithm for the respective frequency of the map shown above. The ellipse in each map represents the acoustic domain for a Mach number of 0.83.

At both frequencies, different sources can be seen to dominate the spectrum. At $f = 750$ Hz mostly a single source is visible in the center of the acoustic domain, where at $f = 1\,758$ Hz the convective ridge dominates the wavenumber spectrum. Applying the FISTA deconvolution reduces significantly the source size and the whole noise level for both frequencies. In addition, the convective ridge ($f = 750$ Hz) and acoustic source structures ($f = 1\,758$ Hz) previously obscured by noise and side lobes can now be clearly

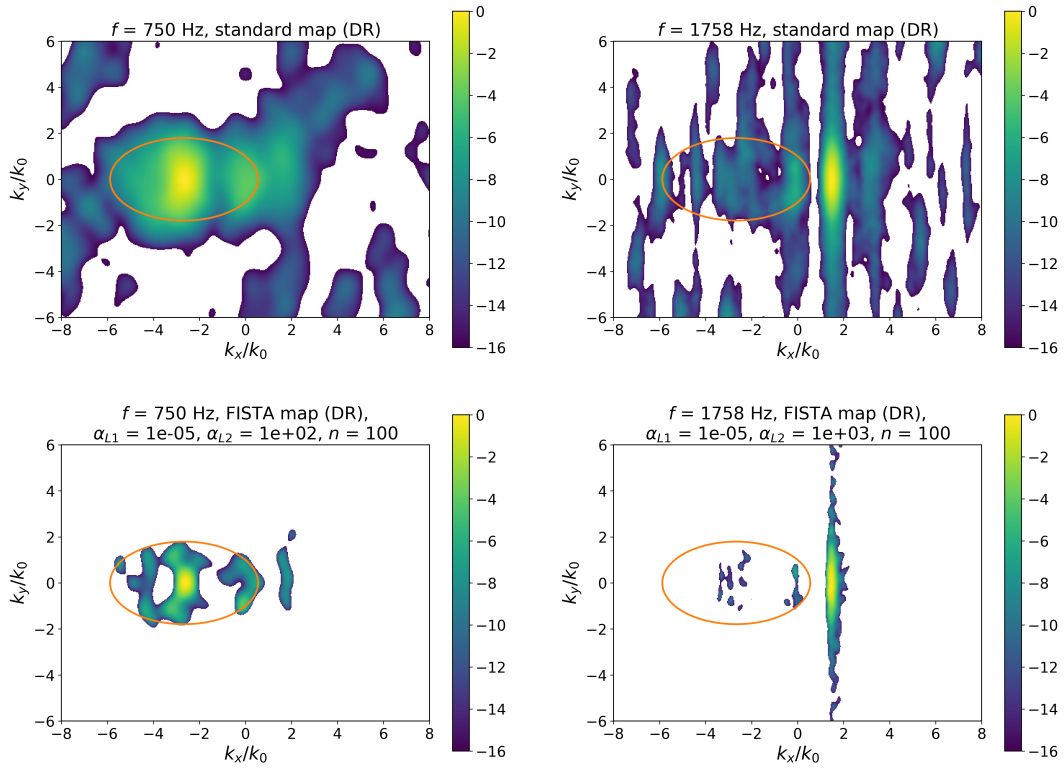

Figure 1: Standard (top) and FISTA (bottom) source maps with diagonal removal applied for $f = 747$ Hz (left) and $f = 1758$ Hz (right). The ellipse marks the border of the acoustic domain.

identified. Relative to the acoustic domain, two main sources can be identified. One source is located approximately in the center, indicating waves parallel to the array. This can probably be attributed to the small dimensions of the test section (1.0 m x 1.0 m) and the associated reflections and standing wave field. Another source appears on the right-hand side of the acoustic domain, probably related to sound sources at the trailing edge, traveling upstream over the array. Also, the structure of the convective ridge seems to be slightly asymmetric. Even so that the properties of the structures can be studied in more details, the influence of the applied FISTA convolution method on the wavenumber shape has to be studied more deeply.

The computation time for 100 iterations and 262 144 focus points was about 25 s per frequency line on an office computer (Python script - only one CPU core used).

Due to short calculation time (compared to DAMAS) and the stable unique solution this algorithm promises to become the standard for wavenumber spectra analysis (at the DLR). All ghost sources or side lobe are reduced dramatically reduced, This leads to an improved separation acoustic and convective parts, more precise determination of the location and shape of the convective ridge.

References

[1] K. Ehrenfried and L. Koop, “Pressure fluctuations beneath a compressible turbulent boundary layer,” in *14th AIAA/CEAS Aeroacoustics Conference (29th AIAA Aeroacoustics Conference)*, 2012.

[2] H.-G. Raumer and C. Spehr, “Wavenumber spectrum determination for aeroacoustic applications using fista,” in *Inter.noise Glasgow*, 2022.

[3] A. Beck and M. Teboulle, "A fast iterative shrinkage-thresholding algorithm for linear inverse problems," *SIAM journal on imaging sciences*, vol. 2, no. 1, pp. 183–202, 2009.

Reduced-order modelling of flow-induced vibration from turbulence impingement

Kostantinos Tsigklifis[1,2], Marcus H. Wong[1], Paul G. Dylejko[1*], Mahmoud Karimi[3], Paul Croaker[1] and Alex T. Skvortsov[1]

[1] Defence Science and Technology Group, Australia

[2] YTEK Pty Ltd, Level 1, 231 High St, Ashburton, Australia

[3] Centre for Audio, Acoustics and Vibration, University of Technology Sydney, Australia

This paper discusses reduced-order modelling approaches to predict the structural vibrations of a flexible cantilever hydrofoil in the presence of incident turbulent flow. The turbulent inflow generates unsteady loading at low frequencies which may lead to excessive noise and structural fatigue. While this problem has been previously studied in-depth [1-4 amongst others], the inclusion of foil flexibility in analytical models has not been as widely reported [5].

The dynamic equations for a hydrofoil may be written compactly as,

$$\boldsymbol{\mathcal{D}}(\eta, z, \omega)\boldsymbol{x} = \boldsymbol{L_G}(GRF, \Psi_{ww}, z,\ \omega\ ) + \boldsymbol{L_{HP}}(T(\kappa), M_c, z, \omega)\boldsymbol{x}. \quad (1)$$

In equation 1, the left side is the structural response and right side are the forcing functions. The operator $\boldsymbol{\mathcal{D}}$ describes the bending and torsional motion of the foil, while $\boldsymbol{x}$ represents the resultant vertical h and angular ϕ displacements. Using 2D hydrofoil theory, the unsteady lift and moment response of a hydrofoil section may be described by superimposing two forcing functions $\boldsymbol{L_G}$ and $\boldsymbol{L_{HP}}$. The forcing function $\boldsymbol{L_G}$ arises from the leading edge of a rigid hydrofoil interacting with an incoming upwash gust and is described by an appropriate gust response function (GRF). On the other hand, using Theordorsen's function $T(\kappa)$ at reduced frequency κ, $\boldsymbol{L_{HP}}$ encapsulates the fluid forces due to the heaving (bending) and pitching (torsion) motion of the hydrofoil section. In hydrodynamic applications, loss mechanisms (η) and added mass (M_c) due to fluid loading effects also need accurate representation. Furthermore, an appropriate model for the spatial correlation function for homogeneous isotropic turbulence (Ψ_{ww}) is required.

Choosing the appropriate technique to solve equation 1 is not straightforward and numerous options have been previously proposed. To not limit ourselves to one technique, we will focus on the correlation method [2], spectrum or wavenumber method [3] and a relatively new deterministic technique known as Uncorrelated Wall Plane Wave (UWPW) [4]. The methods will provide the modelling framework to help test the sensitivity of the important modelling choices (namely $\eta, M_c, GRF, \Psi_{ww}$). Hence, the aim of this work is to provide a clearer path and direction on how to model flexible hydrofoils encountering turbulence.

We restrict our analysis to a single hydrofoil of chord c in water with a freestream velocity U having homogenous turbulence. The foil, at zero degree angle of attack, is divided into M chordwise strips and excited by an appropriate gust U_G at frequency ω. The spanwise distribution is kept constant (though this may be relaxed). Focusing only on the lower-order modes, the structural response $\boldsymbol{\mathcal{D}}$ is adequately described by the Euler-Bernoulli model. Appropriate expressions for both structural and hydrodynamic damping as well as fluid loading terms are included. The resultant vertical h and angular ϕ displacements may be computed by solving the coupled system of equations with appropriate boundary conditions. Figure 1 shows

*corresponding author: paul.dylejko@defence.gov.au

a schematic of the problem with key dimensions. To compare the efficacy between the different modelling choices, the spatially-averaged structural velocity spectra $\overline{S_{uu}}(\omega) = \frac{\sum_{m=1}^{M} S_{uu}(z_m,\omega)}{M}$ of the whole hydrofoil is examined.

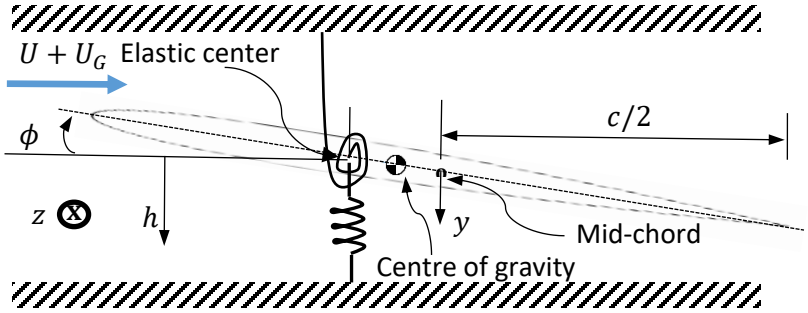

Figure 1: Schematic of a single hydrofoil strip in response to incoming turbulence

The unsteady lift and spatially-averaged structural velocity spectra predicted by the three different methods are shown in figure 2. While there is agreement across all models for the first mode, a variation in amplitude is observed for the higher-order modes.

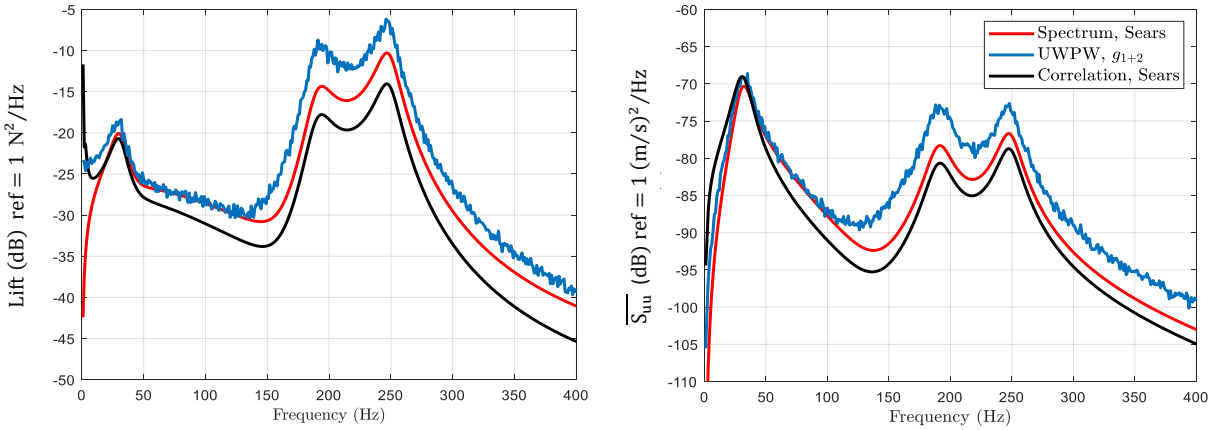

Figure 2: Lift (left) and spatially-averaged structural velocity (right) spectra of a cantilevered NACA0015 hydrofoil predicted by the three different reduced-order models for $U = 5$ m/s

References

[1] W. K. Blake and L. J. Maga, "On the flow− excited vibrations of cantilever struts in water. I. Flow− induced damping and vibration," *The Journal of the Acoustical Society of America* 57.3 pp. 610-625, 1975.

[2] M. R. Catlett and J. M. Anderson, "Modeling unsteady lift on a hydrofoil due to the ingestion of turbulence and hydro-elastic motion." in *proceedings of the 46th AIAA Fluid Dynamics Conference*, 13 – 17 June, Washington, D.C., 2016.

[3] M. Roger and S. Moreau, "Extensions and limitations of analytical airfoil broadband noise models," *International Journal of Aeroacoustics*, 9, pp.273-305, 2010.

[4] M. Karimi, P. Croaker, A. Skvortsov, L. Maxit and R. Kirby, "Simulation of airfoil surface pressure due to incident turbulence using realizations of uncorrelated wall plane waves," *The Journal of the Acoustical Society of America* 149.2 pp. 1085-1096, 2021.

[5] K. Tsigklifis, M. Wong, S. De Candia, P. Dylejko, P. Croaker and A. Skvortsov, "Reduced order modelling of vibroelastic response of a hydrofoil in homogeneous isotropic turbulence," *Proceedings of Acoustics 2021*, 21-23 February, Wollongong, NSW, Australia, 2022.

Fluid-acoustic interactions with resonance around an axial fan in a duct

Hiroshi Yokoyama[1]

[1]Department of Mechanical Engineering, Toyohashi University of Technology
1-1 Hibarigaoka, Tempaku-cho, Toyohashi, Aichi 441-8580, Japan
Email: h-yokoyama@me.tut.ac.jp

Small axial fans are widely used to cool electric devices including personal computers and video cameras. The miniaturization of the electric devices leads to the installation of the fans in a narrow space or duct. For a small axial fan or compressor in a narrow duct, acoustic mode can be generated in the duct [1]. The interactions between intense acoustic resonance and vortex shedding in flows around a static cascade of flat plates were presented in the literatures [2,3]. However, the effects of acoustic resonance on the flow around a fan with rotating blades have not been sufficiently investigated. In the present research, experiments and direct aeroacoustic simulations were performed to clarify the condition for the intense acoustic resonance and the influence of the acoustic resonance on the flow and acoustic fields around a small axial fan in a duct. Another objective is the establishment of the reliable computational methods to directly predict the aeroacoustic fields for a rotational fluid machinery at a low Mach number.

The experiments and computations were performed for the fan with five blades ($Z_b = 5$) in a casing with slits as shown in Fig. 1(a), where the side length of the square outer dimension of the casing was D = 40 mm. The fan was installed in the duct with a square cross section as shown in Fig. 1 (b), and the side length of the duct was set to $H/D = 2.0$ and 4.0. The flow field at the flow coefficient of $\phi \approx 0.17$, where the effects of the duct width on the fan pressure rise became larger, was mainly investigated. The rotational

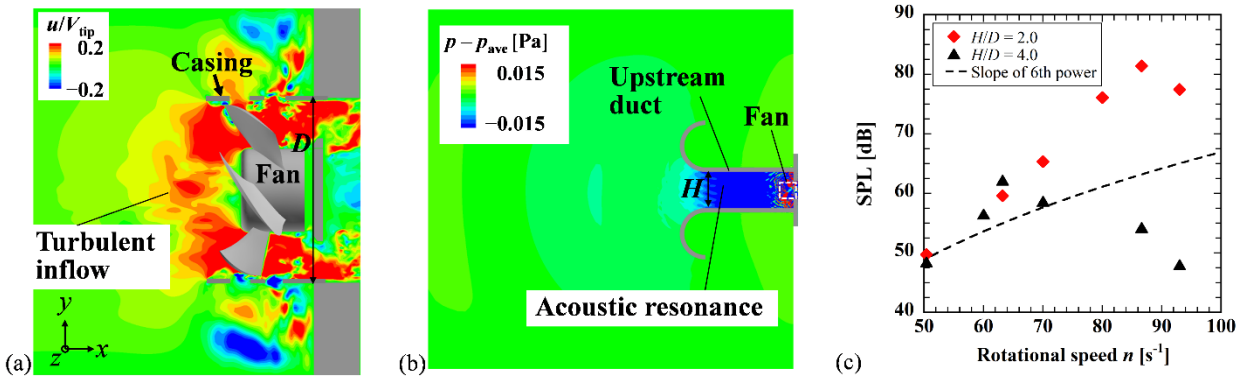

Figure 1: Flow and sound around the fan in a duct (n = 86.6 s^{-1}). (a) Predicted contours of axial velocity normalized by tip velocity near the fan (H/D = 2.0, ϕ = 0.165). (b) Predicted contours of fluctuation pressure around the duct (H/D = 2.0, ϕ = 0.165) , where a region enclosed with a white dotted line is that of Fig.1(a). (c) Measured sound pressure level at the blade passing frequency (2.5D upstream from the fan) for H/D = 2.0 and 4.0 (ϕ = 0.17).

speed n was varied from 50.4 to 93.0 s^{-1} to clarify the condition of intense acoustic resonance. The Mach number based on the blade tip velocity was 0.029, and the Reynolds number based on the chord length was 1.5×10^4. In the simulation, both flow and acoustic fields were directly predicted by the compressible flow simulations. The rotating fan and casing shape were reproduced with a volume penalization method [4]. The computational methods were validated by comparing the predicted static pressure rise and aerodynamic sound by the fan with those measured.

Fig. 1(c) shows the predicted sound pressure level at the blade passing frequency (2.5D upstream from the fan) for H/D = 2.0 and 4.0 (ϕ = 0.17). The sound pressure level became most intense for the specific rotational speed of n = 86.6 s^{-1} for the narrower duct of H/D = 2.0. The predicted contours of fluctuation pressure in Fig. 1(b) show that the acoustic resonance with a one-quarter wavelength mode occurs in the duct. In this condition, flow disturbances were found to occur near the curved wall of the bell-mouthed inlet of the upstream duct due to intense acoustic velocity fluctuations, which prompt the inflow turbulence to the fan as shown in Fig. 1(a). To elucidate the effects of the acoustic resonance on the flow around the fan, the computation with the artificially suppressed acoustic resonance was also performed and the predicted flow fields were compared with those with intense acoustic resonance for the same rotational speed and duct width. The incoming flow to the fan becomes more turbulent when the acoustic resonance occurs, which promotes the spreading of the tip vortices between rotor blades. As a result, the blade loading decreases and the turbulence in the blade wake leading to mixing loss becomes intense, causing the static pressure rise by the fan to decrease. This is consistent with the observed decrease of the pressure rise at the rotational speed for the intense acoustic resonance.

Acknowledgements

This work was supported by MEXT as a Program for Promoting Research on the Supercomputer "Fugaku" (hp200123, hp200134), and JSPS KAKENHI 21K03874.

References

[1] J. M. Tyler and T. G. Sofrin, "Axial flow compressor noise studies," *SAE Transactions*, vol. 70, pp.209–332, 1962
[2] R. Parker, "Resonance effects in wake shedding from parallel plates: Some experimental observations," *Journal of Sound and Vibration*, vol. 4, no. 1, pp.62–72, 1966
[3] H. Yokoyama, K. Kitamiya, and A. Iida, "Flows around a cascade of flat plates with acoustic resonance," *Physics of Fluids*, vol. 25, no. 10, 106104, 2013
[4] H. Yokoyama, K. Minowa, K. Orito, M. Nishikawara, and H. Yanada, "Compressible simulation of flow and sound around a small axial-flow fan with flow through casing slits," *Journal of Fluids Engineering, Transactions of the ASME*, vol. 142, no. 10, 101215, 2020